

# Exceptional 2023 marine ~~heat wave~~ ~~heatwave~~ reshapes North Atlantic coccolithophore blooms

Thibault Guinaldo<sup>1</sup> and Griet Neukermans<sup>2,3</sup>

<sup>1</sup>Centre National de Recherches Météorologiques, Université de Toulouse, Météo-France, CNRS, Lannion, France

<sup>2</sup>Ghent University, Biology Department, MarSens Research Group, Krijgslaan 281 – S8, 9000 Ghent, Belgium

<sup>3</sup>Flanders Marine Institute, InnovOcean Campus, 8400 Ostend, Belgium

**Correspondence:** Thibault Guinaldo (thibault.guinaldo@meteo.fr)

**Abstract.** The North Atlantic ~~Ocean~~ is undergoing rapid ~~transformation driven by~~ ~~ecological evolution under the influence of both~~ long-term warming and the increasing frequency of extreme marine heatwaves. In 2023, ~~surface temperatures across the basin reached record highs, raising concerns about the resilience of phytoplankton ecosystems. This study examines the response of *Emiliania huxleyi*, a key calcifying phytoplankton species, using the North Atlantic experienced record-breaking~~ sea surface temperature anomalies, exceeding +5°C regionally and lasting several months. Using 25 years of satellite-derived ~~ocean colour data. The particulate inorganic carbon data (1998–2023) marine heatwave significantly disrupted bloom intensity and phenology, revealing contrasting trends between two bloom regions. While~~ we assess the response of coccolithophores blooms across two biogeographical boundaries: the Celtic Sea and the Barents Sea. We show that the 2023 MHW led to reduced bloom intensity and ~~extent declined fragmentation~~ in the Celtic Sea, ~~conditions while leading to record-high intensity and extent~~ in the Barents Sea ~~became increasingly favorable for growth. These shifts reflect the immediate impacts of the heatwave superimposed on~~ ~~These contrasting responses are modulated by~~ long-term environmental changes, influenced by processes such as Atlantification, sea-ice retreat, and vertical stratification. The resulting changes have critical implications for carbon cycling and trophic interactions, underscoring the need for sustained, high-resolution monitoring to track both extreme events and persistent trends in phytoplankton dynamics. As high-latitude regions emerge as potential refuges, their long-term stability is highly uncertain under continued warming, ocean acidification, and ecosystem restructuring. A deeper understanding of these dynamics is essential for predicting future carbon cycle feedbacks and for managing ocean ecosystem services in a rapidly changing climate. SST trends, upper-ocean stratification, and polar front shifts. Our findings suggest a spatial shift of coccolithophore blooms with potential implications for the carbon cycle under long-term warming and stratification.

*Copyright statement.* TEXT

## 20 1 Introduction

~~Under specific oceanic and radiative conditions~~ During boreal spring and summer, large parts of the North Atlantic Ocean are transformed into shades of color, ~~signaling~~ indicating the occurrence of phytoplankton blooms. Among these, ~~the coccolithophore~~

*Emiliania huxleyi* forms extensive blooms, typically in summer months, that play a crucial role in oceanic biogeochemical cycles (Shutler et al., 2010) coccolithophores, particularly *Gephyrocapsa huxleyi* (Bendif et al., 2023) the most abundant species, 25 forms extensive summer blooms, which may weaken the ocean sink for atmospheric carbon dioxide (Shutler et al., 2010; Kondrik et al., 2010). During the decline phase of these blooms, the overproduction and detachment of its calcite plates (coccoliths) color the surface waters a distinctive milky-turquoise, detectable by ocean color satellites (Tyrrell et al., 1999; Smyth et al., 2002). In these 30 conditions, coccoliths can contribute up to 90% of the total particulate backscattering coefficient,  $b_{bp}$ , a major determinant of ocean color reflectance (Baleh and Mitchell, 2023). As a photosynthetic organism, *E. huxleyi* contributes an estimated optical satellite sensors (Ackleson et al., 1988; Moore et al., 2012; Neukermans and Fournier, 2018). As photosynthetic organisms, coccolithophores contribute 1-10% of global primary production, underscoring its importance in the context of anthropogenic-driven ocean warming and acidification. *E. huxleyi* is also an important contributor to the oceanic stock and downward to global ocean primary production (Poulton et al., 2007) and about 50% to the deep ocean flux of particulate inorganic carbon (PIC), and a key player in the oceanic carbon cycle, influencing (PIC; Neukermans et al., 2023). Coccolithophores thus contribute to both 35 the organic carbon pump and the carbonate counter pump mechanisms (Neukermans et al., 2023). Finally, coccolithophores play a significant role in the production of the volatile sulfur-containing compound dimethylsulfide (DMS, Malin et al., 1993) are a major producer of dimethylsulfide (Malin et al., 1993), that can promote the formation of marine clouds with important implications for climate regulation (Fiddes et al., 2018; Mahmood et al., 2019).

40 Due to their resilience in low nutrient conditions, coccolithophore dynamics are expected to be driven by ocean warming and stratification, as evidenced by their poleward shift in response to rising sea surface temperatures (SSTs) (Meyer and Riebesell, 2015; D'Amato et al., 2015). Optical satellite observations, available since the late 1970's, reveal a poleward expansion of *G. huxleyi* blooms (Winter et al., 2014), at a particularly rapid rate in the Barents Sea (Neukermans et al., 2018). This shift, associated with an increased occurrence in the North Atlantic (Rivero-Calle et al., 2015) is leading to regional changes in carbon export and ocean alkalinity (Hutchins and Tagliabue, 2015). 45 While bio-advection and atlantification of *G. huxleyi* blooms may be driven by increased advection of water masses contribute significantly to this poleward migration (Oziel et al., 2020), the inhibitory effects of ocean acidification may limit coccolithophore calcification in the Arctic, despite the region's rapid warming (Smith et al., 2017). However, the resilience and adaptive capacity of coccolithophores suggest that they may be able to persist and even flourish under changing environmental conditions (Schlüter et al., 2014) in which *G. huxleyi* is already established (Oziel et al., 2020), and/or by improved blooming conditions 50 toward higher latitudes, including increasing water temperatures (Winter et al., 2014; Beaugrand et al., 2013; Rivero-Calle et al., 2015; Neukermans et al., 2018), or increasing water column stratification giving competitive advantages for *G. huxleyi* (Neukermans et al., 2018).

Over the past 40 years, oceans have absorbed approximately 91% of excess anthropogenic anthropogenic excess heat (Von Schuckmann et al., 2020), leading to significant increases in ocean heat content and raising concerns about an accelerated warming (Li et al., 2023; Minière et al., 2023). Globally, SSTs have risen by an average of 0.97 $\pm$ 1.0°C (confidence interval: 0.77°C – 1.09°C) between 1850-1900 and 2014-2023 (Forster et al., 2024) 2015-2024 (Forster et al., 2025). This long-term warming trend, combined with internal variability, results in anomalously high SSTs known as marine heatwaves (MHW,

Hobday et al., 2016; Oliver et al., 2021). These events have become more frequent and intense, with the North Atlantic emerging as a hotspot, particularly at high latitudes (Oliver et al., 2018). ~~Despite a surface signature, these~~ These extremes can extend vertically and increase environmental pressure on marine ecosystems altering trophic functions, thus leading to economic impacts (Smith et al., 2021, 2023). These ~~consequences~~ effects are exacerbated by a combination of ~~hazards arising from different sources~~ biogeochemical or atmospheric conditions known as compound events (Zscheischler et al., 2018; Burger et al., 2022; Le Grix et al., 2022). ~~These conditions can cause~~ causing an irreversible state for marine communities ~~in a short to medium-term period even in the context of overshooting~~ (Santana-Falcón et al., 2023) (Santana-Falcón et al., 2023; Wernberg et al., 2025).

65 .

### ~~The North Atlantic ocean~~

~~The Atlantic Ocean~~ has experienced some of the most pronounced ocean heat content increases (Cheng et al., 2022) ~~. In recent years, the superposition of this underlying warming trend with extreme internal variability that~~ has led to unprecedented marine heat extremes, particularly affecting the ~~North West European Shelf~~ (Fig. 1a; Guinaldo et al., 2023; Simon et al., 2023). 70 ~~Northwest European Shelf~~ (Fig. 1a; Guinaldo et al., 2023; Simon et al., 2023). In 2023, a record-breaking ~~MHW developed~~ marine heatwave developed, resulting in SST anomalies exceeding  $+5^{\circ}\text{C}$  across broad areas of the shelf ~~for 16 days~~ in June (Berthou et al., 2024). In fact, the entire North Atlantic has reached record-level SSTs explained by anomalies in the air-sea ~~fluxes enhanced heat fluxes, amplified~~ by anthropogenically driven stratification of the upper ocean (Guinaldo et al., 2025). Knowledge about the global causes and consequences of MHWs have increased significantly in recent years (Sen Gupta et al., 2020; Capotondi et al., 2025) with several studies documenting and shoaling of the mixed layer depth (MLD; Guinaldo et al., 2025; England et al., 2025). Several studies have assessed the causes of MHW and their impacts on phytoplankton communities based on chlorophyll-a measurements (Sen Gupta et al., 2020; Capotondi et al., 2024) and some have documented impacts of MHWs on phytoplankton blooms using remotely sensed chlorophyll-a observations (Cheung and Frölicher, 2020; Arteaga and Rousseaux, 2023; Cyr et al., 2024). ~~This study aims at providing a comprehensive assessment of the impacts of the~~ In this study, we investigate 80 ~~how the extreme~~ 2023 ~~North Atlantic exceptional MHW on coccolithophore blooms, a less-studied but ubiquitous taxon in this region using the long-term MHW event impacted coccolithophore bloom dynamics across the North Atlantic Ocean, using remotely sensed PIC observations. We focus on two biogeographical limits, the Celtic Sea and the Barents Sea, respectively representing the trailing (or equatorward) edge and the leading (or poleward) edge of *G. huxleyi* bloom distribution in the North Atlantic Ocean~~ (Winter et al., 2014). Using 25 years of ocean colour satellite data ~~record (1998–2023) as a baseline (1998–2023)~~, we assess changes in the phenology of *G. huxleyi* blooms (including timing and intensity), as well as spatial extent, and contextualise them within long-term trends.

## 2 Results

### 2.1 Environmental conditions

~~Figure 2 illustrates the temporal evolution of SST To evaluate the impact of MHW on *G. huxleyi* blooms, we examine impacts on the three most influential environmental variables that characterize the ecological niches of coccolithophore species, namely~~

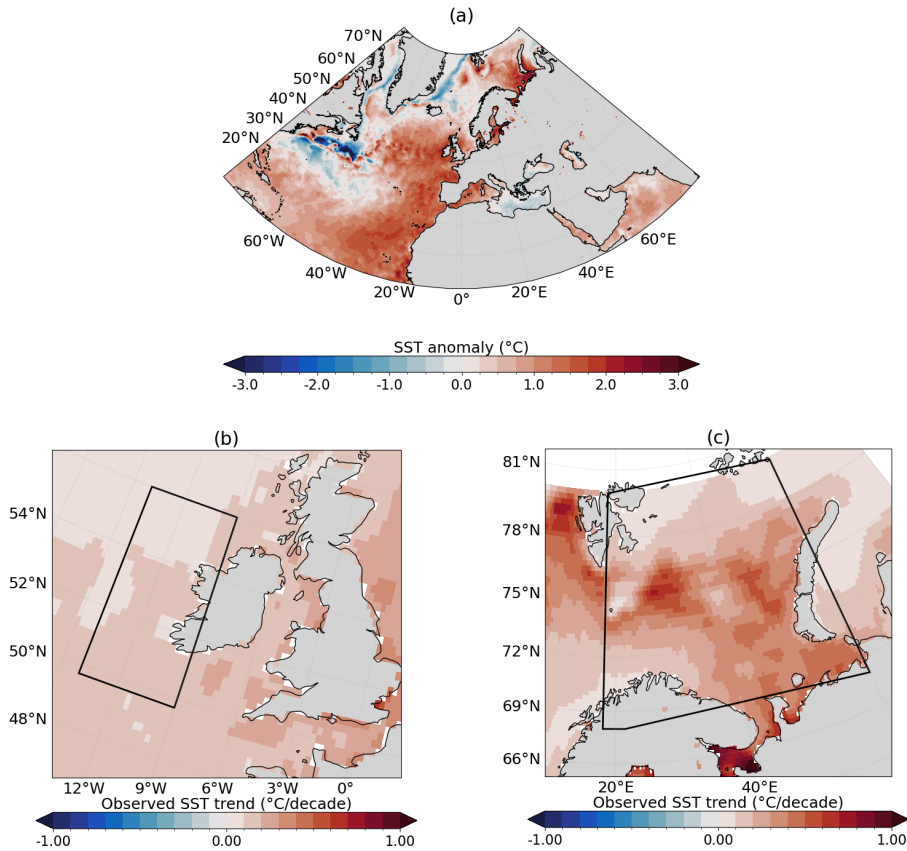


**Figure 1. Maps of SST anomalies for May-June 2023 in the North Atlantic and SSTs trends over the study sites.** (a) May-June averaged SSTs anomalies compared to the corresponding 1991-2020 period. Observed SST linear trend expressed in Celsius degrees by decade, computed from OSTIA over the period 1958-2023 for (b) the Celtic Sea and (c) the Barents Sea. Black boxes indicated the study sites chosen.

SST, Photosynthetically Active Radiation (PAR), and the depth of the mixed layer (MLD), an indicator for the water column stratification (see Sect.A1.4; O'Brien et al., 2016). For *G. huxleyi*, the optimal SST range was found to be situated between 6 and 16°C, optimal PAR between 35 and MLD in the Celtic Sea (CS) 42 Einstein.m<sup>-2</sup>.day<sup>-1</sup>, and optimal MLD between 20 and Barents Sea (BS) during 2023. Both basins experienced record-breaking MHWs starting in spring. The annual mean SST anomaly was 30 m (O'Brien, 2015). These ranges were extracted from the realized ecological niche of *G. huxleyi* (i.e. the environmental conditions under which it can be observed) set up by O'Brien (2015), based on a global compilation of in situ measurements of coccolithophore species abundance and diversity (O'Brien et al., 2013).

In 2023, both the CS and BS experienced exceptional MHWs beginning in spring (Fig.2a-b). Annual mean SST anomalies reached +0.67°C in the CS, peaking in June, and +0.92°C in the BS, peaking in August. Daily Maximum daily SST anomalies reached a maximum value of 17.5+3.9°C (anomaly: +3.9 corresponding to 17°C) in CS and 8.8+3.3°C (anomaly: +3.3 corresponding

to 8.8°C) in BS ~~with warmer SSTs locally~~.

These MHWs were exceptional in ~~both~~ intensity and duration, ~~persisting for~~ ~~lasting~~ 82 days in the CS and 120 days in the BS.

This ~~record-breaking year in the northeastern Atlantic aligns with a global context of extreme heat events occurrence in spring 2023 (Guinaldo et al., 2025)~~ on top of the ongoing warming trend in these basins occurred in a context of unprecedented global

105 ocean heat anomalies (Terhaar et al., 2025) with a particular warming signature over the North Atlantic ocean (England et al., 2025; Guinaldo . These events were boosted by the long-term warming trend, particularly in the BS, where the warming trend is more than twice the global average (Fig.1b-ec).

110 ~~The mixed-layer depth (MLD) in both basins followed a seasonal cycle~~ Likewise, PAR in CS was strong in May-June with values surpassing 42 Einstein.m<sup>-2</sup>.day<sup>-1</sup> (upper-range of the optimal conditions for *G. huxleyi* with thresholds established from the study of the species' realized ecological niche; see Sect.A1.4 and O'Brien (2015)) with conditions becoming more favorable in July onward (Fig.2c). These variations are primarily influenced by the atmospheric conditions, specifically cloud cover. In June, a persistent high-pressure system over Fennoscandia (Fig.A1) led to exceptionally weak wind conditions (Fig.A2) and low cloud cover (Fig.A3) but increased toward climatological values onward . In BS, PAR was exceptionally high compared 115 to the summer climatology allowing sufficient sunlight to reach the surface ocean for photosynthesis throughout summer (Fig.2d). These results are influenced by the cloud cover over BS where a large portion of the sea experienced significant clear-sky conditions during summer (Fig.A3).

120 In 2023, MLD dynamics followed the usual seasonal cycle in both basins, with winter deepening and summer shoaling, ~~with deeper mixing in winter and shallower MLD in summer~~, modulated by atmospheric conditions (Fig. 2, de Boyer Montégut et al., 2004) . The seasonal MLD pattern reflects the variability of mid- and high-latitude climate driven primarily by the (de Boyer Montégut et al., 2004) . In winter, the North Atlantic Oscillation (NAO) ~~in winter~~, which enhances westerly winds and cyclonic conditions (Hurrell et al., 2003) . Enhanced vertical mixing and advection during this period lead to deeper MLD drives vertical turbulent mixing through westerlies and increased storm activity (Hurrell et al., 2003). Even at the northern edge of the North Atlantic, BS climate 125 variability is influenced by the NAO which enhances heat transport (Sandø et al., 2010). Conversely, during summer , the climate variability is reduced, with increased the BS atmospheric and oceanic internal variability responds to NAO conditions (Levitus et al., 2009; Chafik et al., 2015), while summer conditions favor the likelihood of high-pressure blocking systems . These atmospheric conditions, characterized by low wind and high incoming solar radiation , promote upper-layer ocean warming, stratification, and over northern Europe (Rantanen et al., 2022; Rousi et al., 2022) characterized by weak winds and high solar radiation (Fig.A1 & Fig.A2 & Fig.A3). These favour upper-ocean warming, weak winds and shallow MLD, leading 130 to MHW development (Holbrook et al., 2020). In high-latitude regions, additional stratification is driven by sea-ice melting and freshening of the surface waters (Oziel et al., 2017). This relation is particularly visible in CS during June where the upper-ocean remained stratified in response to the consequences of the persistent high-pressure systems (Fig.A1).

135 In the CS, ~~oceanic conditions remained favorable for coccolithophores until~~ SSTs remained around 13°C from May to mid-June, ~~coinciding with the peak of June MHWs~~. From mid-June to mid-July, SSTs ~~exceeded~~ in the optimal thermal range

for *G.huxleyi* blooms (6°C-16°C, see Sect.A1.4 & Fig.2a). However, from June onwards SSTs frequently exceeded 16°C, with localized peaks over 20°C at the peak of the upper thermal range of *E.huxleyi* (O'Brien, 2015) while the second half of summer was marked by destratification associated with the MHW (Berthou et al., 2024). This period was followed by a temporary deepening of the MLD greater than 40m due to the return of westerly winds -in July and August (Fig. A2). A 140 second MHW occurred in September, linked to a high-pressure blocking system and developed in September associated with the return of favorable conditions for blooms ended with the deepening of the MLD. In contrast both SST and MLD (< 40m) to favorable bloom conditions.

Conversely, the BS exhibited a less variable pattern, with favorable conditions persisting from mid-July less temporal variability throughout summer and maintained temperature within the 6°C-16°C range (summer mean: 6.8°C) and exhibited persistent 145 shallow MLD (summer mean : 18 m) consistent with weaker than normal or close to the normal winds (Fig.A2), providing sustained conditions favorable for bloom development from July to early October, -primarily driven by the stratification dynamic.(Fig. 2b, see Sect.A1.4).

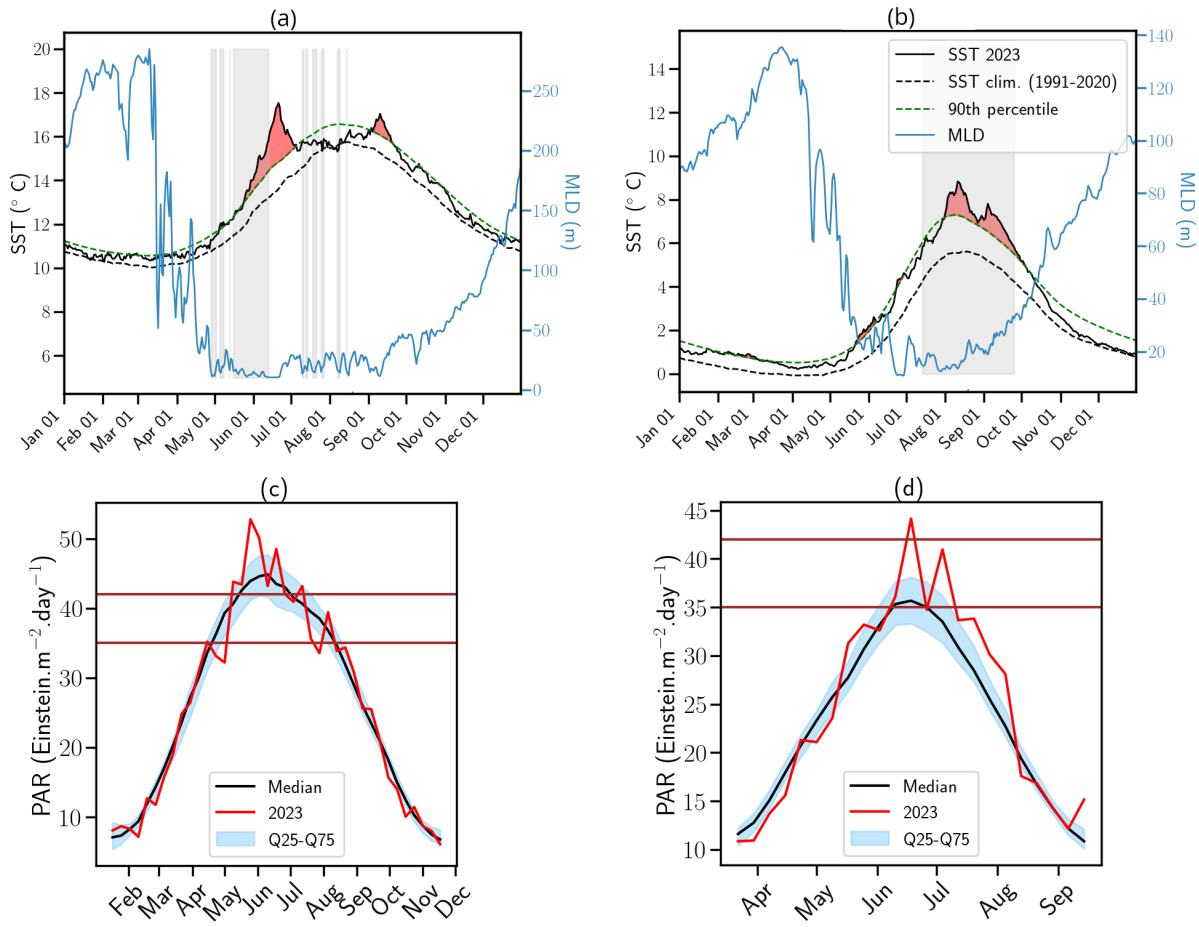


**Figure 2. Daily spatially averaged SST and MLD variables for 2023. Daily spatially averaged SST, MLD and PAR variables for 2023.** Spatially averaged sea surface temperature (SST) (black solid line) and mixed-layer depth (MLD) (blue solid line) anomalies for 2023 in (a) the Celtic Sea and (b) the Barents Sea. The black dashed line represents the climatological SST averaged over each basin for the period 1991–2020, while the green dashed line marks the 90<sup>th</sup> percentile threshold for marine heatwaves (MHWs), as defined by Hobday et al. (2016) (Hobday et al., 2016). Red shading indicates periods of MHWs, while grey shading highlights conditions conducive favorable to *E. huxleyi* blooms based on optimal ranges for SST and MLD thresholds in the species' realized ecological niche (see Sect. A1.4; O'Brien, 2015). Spatially averaged PAR for 2023 in (c) the Celtic Sea and (d) the Barents Sea. The vertical brown lines inform on the optimal range for *E. huxleyi* blooms (see Sect. A1.4).

## 2.2 Bloom dynamics and characteristics

The PIC dynamics reflected these environmental conditions

150 Satellite-derived PIC time series revealed contrasting bloom variations reflecting the SST and MLD conditions in both basins. In the CS, the bloom followed a typical seasonal trajectory, with a climatological rise from April to early June, peaking evolution, intensifying from April, peaking in June at  $0.30 \text{ mmol.m}^{-3}$  (climatology:  $0.30 \text{ mmol.m}^{-3}$  (below the climatological median of

0.43 mmol.m<sup>-3</sup>, <sup>-3</sup>; Fig.3a), followed by a decline over the summer and ending early July. An unusual second bloom occurred secondary bloom emerged in August-September, correlated with the SST anomalies, reaching coinciding with positive SST 155 anomalies and reached 0.38 mmol.m<sup>-3</sup> (−3, above the climatological Q75 : 0.23 (0.24 mmol.m<sup>-3</sup> <sup>-3</sup>, Fig.3a). While similar fall late-summer and fall fall blooms have been observed historically (1997-2022 September maximum September maximum over the 1997-2022 period: 0.61 mmol.m<sup>-3</sup>, Fig.3a & A9 <sup>-3</sup>, Fig.3a), the 2023 bloom was well above the climatological norm. In contrast, the BS exhibited an unprecedented summer bloom. While following the climatological seasonal cycle, this bloom 160 was remarkable in its intensity (6.25 mmol.m<sup>-3</sup> compare to the climatological mean of 1.15 mmol.m<sup>-3</sup>, Fig.3b) and duration, surpassing levels of the previous record set in 2022 (6.15 mmol.m<sup>-3</sup>). This bloom dynamic correlated with the environmental conditions, including MHWs in June and prolonged stratification throughout the summer. The primary limiting factor for blooms in the BS is the photosynthetically active radiation (PAR), which drives bloom onset and decline.

**Coccolithophore bloom phenology and extent in the Celtic and Barents Seas over the satellite record (1998-2023).** Seasonality in satellite-derived PIC concentration in 2023 (red line) compared to the 1998-2020 climatology (black line) in 165 the (a) Celtic Sea and (b) the Barents Sea. Blue (resp. red) dots indicate minimum (resp. maximum) PIC concentration in the 1997-2022 climatology. Grey shading represents the 25-75 interquartile range. Brown lines represents the 10th percentile. Corresponding maximal (yellow bars) and mean (green bars) bloom spatial extent in the (c) CS and (d) BS.

In the CS, the mean summer bloom extent in 2023 reached a record-breaking event exceeded the interquartile climatological 170 range. The 2023 mean bloom surface extent in the CS reached a record 46,460 km<sup>2</sup> (Fig.3c), representing a 30% increase from over the previous record in (2007) and an 85% increase from relative to the 1998-2021 mean. However, the maximum bloom extent (126,163 km<sup>2</sup>) was comparable remained close to the 1998-2010 mean (126,345 km<sup>2</sup>), potentially reflecting the multi-annual North Atlantic variability. The increase in mean bloom extent may be attributed to a prolonged bloom period with smaller blooms unevenly distributed across the CS suggesting persistent but unevenly distributed blooms across the 175 CS (Fig.A4). These levels are anomalously high in 2022 and 2023 (mean surface extent anomaly : 25,551 km<sup>2</sup>; maximal surface extent anomaly: 25,864 km<sup>2</sup>) with a significant correlation with a multi-year trend of increasing spring-summer SSTs (Fig.A4-3e, Fig.Aa & Table A1). The significant correlation between summer SST and bloom extent suggests an important role for sustained surface warming in modulating bloom dynamics in this region.

In the BS, bloom extent exhibited a remarkable rise over the past two years, setting new records in both mean (164,188 km<sup>2</sup>, an exceptional summer bloom in 2023 peaked at 6.25 mmol.m<sup>-3</sup> (much higher than the climatological median value 180 of 1.15 mmol.m<sup>-3</sup>, Fig.3d) and maximum (b), reaching values similar to the previous record set in 2022 (6.16 mmol.m<sup>-3</sup>). The 2023 bloom occurred simultaneously with the development of the MHW in June, providing SST and MLD conditions ideal for blooms (see Sect.A1.4 and Sect.2.1). The bloom extent reached record highs of 833,561 km<sup>2</sup> values for 2023. The latter extent represents an in 2023; much higher than the mean value of 164,188 km<sup>2</sup> and 18% increase from higher than the previous record set in 2022 (of 703,174 km<sup>2</sup>). Spatially, this reflects a significant intrusion of the set in 2022 185 (Fig.3d). This expansion reflects an northeastward intrusion of coccolithophores into the BS (Fig. A), linked to the shifting polar front (Fig.A6, Fig.A7, Neukermans et al., 2018; Oziel et al., 2020), with blooms covering 59% of the basin linked to increased atlantification with favorable bloom conditions. Long-term trends indicate a consistent rise in 2023, a new record

for expansion. Over the past 25 years, LOESS regression reveals significant positive trends in bloom extent, with positive trends of  $3.137 \text{ km}^2 \text{ year}^{-1}$  for the mean and  $12.346 \text{ km}^2 \text{ year}^{-1}$  of the maximum spatial extent (p\_value<0.01) with a record maximum area exceeding by  $392\,000 \text{ km}^2$  the climatological value (Fig.3f).

In the BS, the increase in bloom extent was also significantly correlated with summer SSTs (Fig. Ab, Table A1), highlighting the role of warming in driving these changes. Two distinct processes contribute to this warming: long-term ocean temperature increase, especially pronounced at high latitudes, and enhanced inflow of Atlantic Water ("Atlantification", Árthun et al., 2012). To disentangle these contributions, we tracked the annual position of the polar front, a proxy for Atlantic Water influence (Fig.A7a, Neukermans et al., 2018). While the mean position of the front has shifted approximately 95 km northward since the early 2000s (Fig.A7b), its position has stabilized over the past 25 years two years following a strong southward shift from 2016 to 2020, with extension occurring primarily toward the east rather than the north (Fig.A6 & A7a). In parallel, ocean warming continued, with a long-term trend of  $+0.26^\circ\text{C}$  per decade (Fig.1c & Ab). The 2023 MHW further amplified this trend, producing localized SST anomalies across the BS basin and leading to one of the warmest boreal summer anomalies in the Barents Sea (Fig. Ab). A significant correlation between bloom surface extent and SST (Table A1) confirms the influence of gradual warming and interannual variability on coccolithophore proliferation. However, the polar front is only a proxy of the process of atlantification and weak correlation between the position of the thermal front (western basin : 0.45, as estimated by LOESS regression (p\_value <0.01) 0.05; eastern basin: 0.35, p\_value = 0.07) and the leading edge of coccolithophore bloom distribution (Fig.A8) suggests an important role for SST which should exceed the  $6^\circ\text{C}$  limit for *G.huxleyi* to proliferate.

## 205 2.3 Trends in coccolithophore bloom phenology over the satellite era (1998-2023)

### 2.3 *G.huxleyi* bloom trends in the satellite era (1998-2023)

Basin-averaged analyses may hinder spatial feature can hinder spatial features such as the repartition and the evolution of blooms across each basin. As shown on Figure A4, the summer maximum PIC concentration showed no detectable trend in the CS. However, in the BS Here, we focus on the spatial features of the blooms.

210 In the CS, no significant trend in summer PIC maxima was detected (Fig.A), a strong A9a). In contrast, the BS exhibited a northeastward shift in summer maximum concentrations was observed, aligning with the shifting (Fig.A6 & A8). While the western BS shows limited front variability and no consistent trend, the eastern BS is characterized by high interannual variability and a long-term northward shift of 300 km for the northernmost position of the polar front and thus the atlantification of the water masses. Interannual bloom and a shift of 155 km for the latitudinal mean position of the bloom. Even though 215 the latitudinal mean front position have regressed since 2016, another level close to the record high was reached in 2023 (Fig.A8), exhibiting a spike in the northward maximal expansion in 2022 and 2023 (Fig.A6). This spatial reorganization of plankton distribution in the Barents Sea has been associated with 'Atlantification', which in turn enhances blooms of temperate phytoplankton such as *G.huxleyi* through bio-advection (Oziel et al., 2017). However, this phenomenon does not fully explain the exceptional bloom observed in 2023 even if the interannual variability in the position of the polar front is 220 accompanied by shifts in PIC maxima, likely driven by bio-advection processes transporting particulate material along the

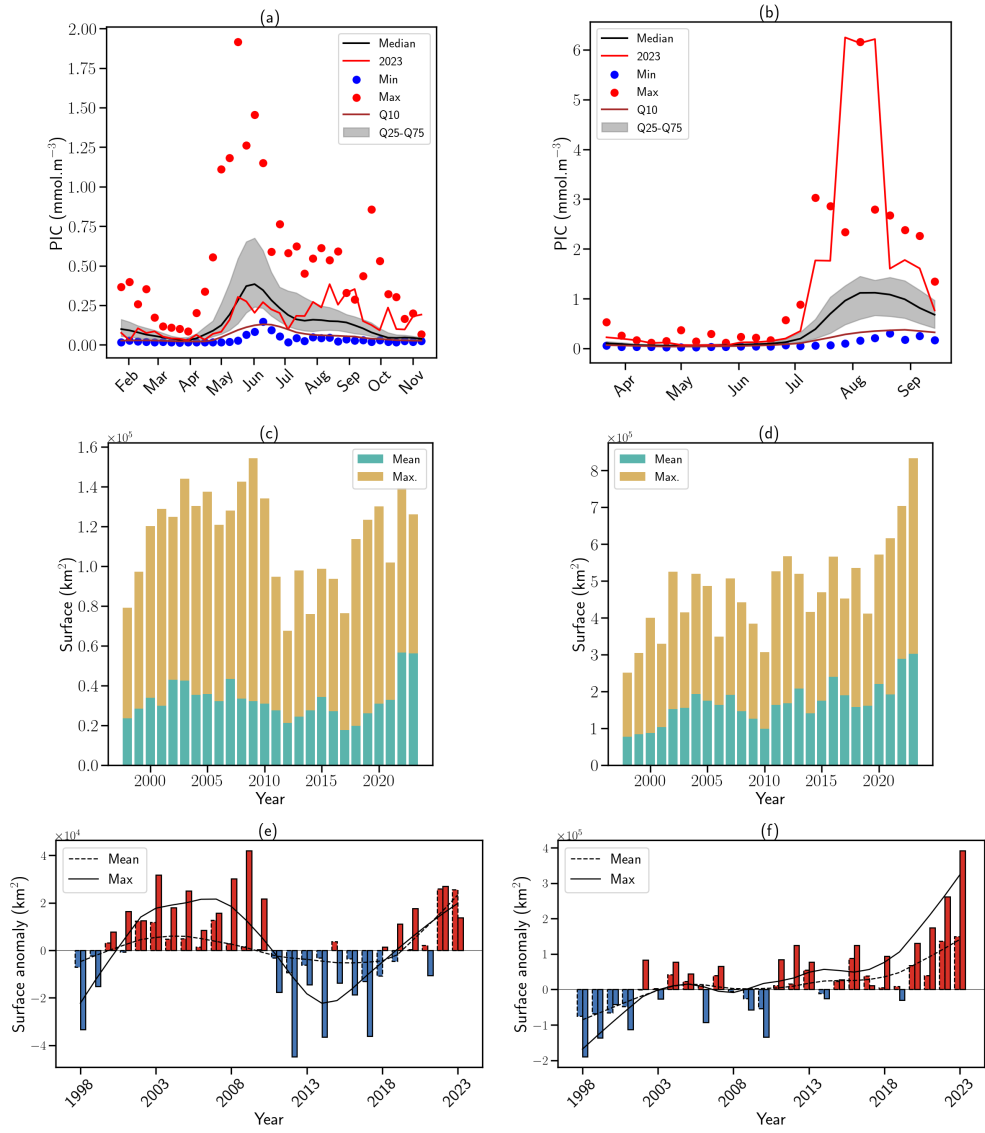


**Figure 3. *G. huxleyi* bloom phenology and surface extent in the Celtic and Barents Seas over the satellite record (1998-2023).** Seasonality in satellite-derived PIC concentration in 2023 (red line) compared to the 1998-2020 climatology (black line) in the (a) Celtic Sea and (b) the Barents Sea. Blue (resp. red) dots indicate minimum (resp. maximum) PIC concentration in the 1997-2022 climatology. Grey shading represents the 25-75 interquartile range. Brown lines represent the 10th percentile. Maximal (yellow bars) and mean (green bars) bloom spatial extent in the (c) CS and (d) BS. Corresponding surface extent anomalies (seasonal mean are in solid contour and seasonal maximum in dashed contour) for (e) CS and (f) BS. Anomalies are computed relatively to the 1998-2018 climatological period. Red bars indicate positive anomalies, while blue bars indicate negative anomalies. The lines indicated the corresponding 10-year LOESS trend.

front (Oziel et al., 2020). Years (e.g. 2004, 2010, and 2023 exhibited larger areas of elevated PIC (Fig.A). This underscores the compound effect of the Atlantification and ocean warming on the shift of optimal conditions and the enhancement of such a situation under extreme MHWs events like in 2023; Fig.A6 & A7 & A9b).

225 **Phenology of coccolithophore blooms in the North-eastern Atlantic ocean (1998–2023).** Start and end dates of blooms with maximum PIC, colored by peak PIC concentration ( $\text{mmol.m}^{-3}$ ) in the (a) CS and (b) the BS.

The phenology of coccolithophore blooms in the CS over the 25-year period exhibited marked interannual variability in bloom peak. Phenological analysis revealed contrasting bloom dynamics in both regions. In the CS, bloom timing, duration, and intensity (see Fig.??a and Section A1). The average bloom duration was and intensity exhibited marked interannual variability (Fig.4a). On average, blooms last 90 days, ranging from 21 to 200 days for the weakest blooms. The mean bloom start date occurred with onset typically in mid-April while the blooms generally ended and decline by mid-July. A significant shift in bloom duration was observed during For the last three years (2021–2023), a remarkable 2021–2023), bloom duration increased by 130% increase in duration relative to the 1998–2020 mean. This trend underscores recent anomalies in seasonal dynamics which is linked with recurrent warm conditions in summer and autumn thus shifting the optimal thermal conditions. The 235 bloom intensity, as measured by the maximum PIC value, averaged  $1.4 \text{ mmol.m}^{-3}$  0.5–3.3 over the study period. Notably, the mean intensity (Fig.4a), reflecting a shift in seasonal conditions due to recurrent late-summer warming (Fig.Aa). However, average peak PIC concentration declined by 20% during the last three years compared to the 1998–2020 period. Despite these interannual variations (2021–2023 average compared to the 1998–2020:  $1.4 \text{ mmol.m}^{-3}$ ). Despite interannual variability, this recent decline seems to confirm imprint a negative trend in bloom intensity over the 25-year period ( $-0.03 \text{ mmol.m}^{-3}$  per 240 year), although this trend is not statistically significant ( $p_{\text{value}} = 0.07$ ) (Fig.A7; Fig.A9a).

In the BS, coccolithophore bloom phenology differed notably to the one in the Celtic Sea. The mean bloom duration was shorter, averaging In contrast, the BS exhibited more consistent bloom timing, with mean bloom durations of 70 days [35–118], with no detectable temporal shift in bloom timing across the 1998–2023 period. The mean start date was consistently around 245 beginning in mid-June, while the mean end date occurred and ending in mid-August mid-June (Fig.4b), reflecting a shorter seasonal window for bloom development. The lack of temporal shifts No temporal trend in bloom timing is evident in Figure ??b, which shows consistent bloom periods across years. Bloom intensity in the BS was significantly higher than in the CS, with a mean maximum PIC value of  $3.9 \text{ mmol.m}^{-3}$  1.2–16. Recent years (2021–2023) demonstrated a notable increase in bloom intensity, culminating in a record daily was detected between 1998 and 2023. However, bloom intensity increased significantly 250 in recent years. A new record daily PIC value of  $16.5 \text{ mmol.m}^{-3}$  was observed in 2023, nearly double the previous daily record of record set in 2022 ( $8.6 \text{ mmol.m}^{-3}$  in 2022). The mean intensity for the last three years was  $\text{mmol.m}^{-3}$ . The mean peak intensity over 2021–2023 reached  $12.5 \text{ mmol.m}^{-3}$ , compared to the  $3.2 \text{ mmol.m}^{-3}$  for the preceding years. This sharp increase  $^{-3}$  over 1998–2020. This surge resulted in a significant positive trend in bloom intensity ( $0.17 \text{ mmol.m}^{-3}$  per year,  $p < 0.05$ ) over the 1998–2023 period, Fig.A9a).

255 Bloom development also depends on upper-ocean stratification, which relates to nutrient and light availability, as well as

mixing. Both the CS and BS exhibit long-term trends toward stronger stratification (Fig. A7b). Further analysis suggests a link between the observed rise in bloom intensity and environmental conditions influenced by Arctic warming ((Fig. A8). Previous studies have shown that reduced sea ice extent and longer ice-free seasons in the Arctic enhance water column stratification, increase light availability, and facilitate the accumulation of nutrients, creating A10 & A11). In the CS, this trend is driven by 260 temperature (Fig. A10), while in the BS, the trend is mostly driven by changes in salinity, with temperature playing a secondary role (Fig. A11). In both regions, 2023 experienced a positive stratification anomaly even being a record year in CS ensuring favorable conditions for coccolithophore growth (Ardyna et al., 2014; Oziel et al., 2016). These processes likely contributed to the unprecedented bloom intensities observed in recent years *G. huxleyi* (see Sect. A1.4).

265 The Together, these contrasting phenological responses in the CS and BS highlight the underscore the influence of regional environmental drivers on coccolithophore bloom dynamics. While the CS exhibited a recent extension of bloom duration and a decline in intensity deviating from typical multi-annual variability, the BS showed stability in bloom timing but an unprecedented increase in bloom intensity. Here, the bloom period remains limited by PAR availability, preventing further lengthening despite significant SST warming trends (Fig. 2e). In the CS, recent anomalies reflect prolonged bloom duration but 270 reduced intensity, whereas in the BS, bloom timing remains stable while intensity increases drastically due to favorable ocean warming and stratification. Whether these changes represent a persistent regime shift remains uncertain at this point and will require analyses of a longer time series.

### 3 Discussions and Conclusions

#### 3 Conclusions

275 The year 2023 was marked by extreme surface ocean temperatures extending across the North Atlantic over a prolonged period. The establishment of these temperatures was locally modulated by climate variability, leading to the onset of historic marine heatwaves (Guinaldo et al., 2025). In particular, the Northeast Atlantic experienced oceanic extremes that were both historically anomalously intense and prolonged (Berthou et al., 2024). Using ocean-colour dedicated satellite sensors, this study demonstrated that these extremes impacted coccolithophore dynamics and enhanced consequences of the long-term warming trend. Specifically, a shift was observed in the optimal bloom development zones during spring-summer, with a degradation of thermal conditions in trailing regions our results reveal how calcifying phytoplankton respond differently at biogeographic limits: degradation at the trailing edge (Celtic Sea) and an improvement in leading regions amplification at the leading edge (Barents Sea) raising concerns about a possible contraction of the blooms optimal areas. However,

285 In the Celtic Sea, the primary bloom was subdued when both SSTs and PAR exceeded the optimal thermal limit of *G. huxleyi* ( $>16^{\circ}\text{C}$ ), and although a secondary bloom developed in late summer, overall bloom intensity declined over the 1998–2023 period. A trend of prolonged but weaker blooms was observed in 2021–2023, combined with increased stratification which may indicate a shift toward less favorable conditions for *G. huxleyi* to bloom.

In contrast, the improved conditions at high latitudes depend on other factors, notably the Atlantification dynamics in the

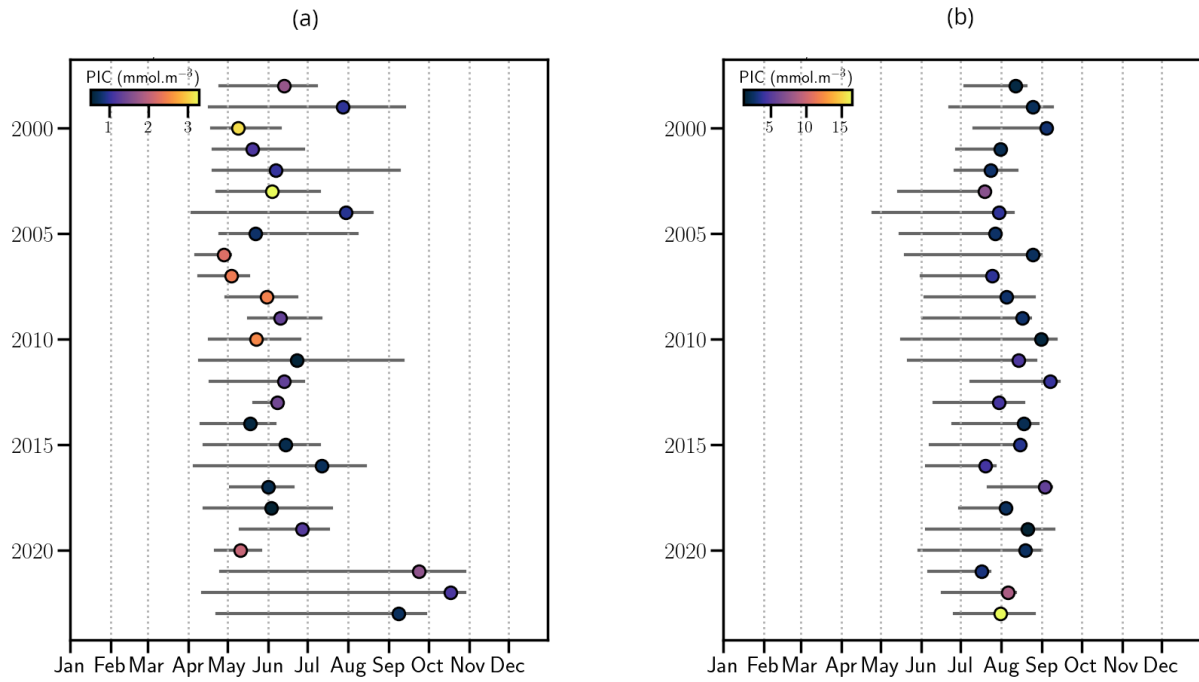


**Figure 4. Phenology of coccolithophore blooms in the North-eastern Atlantic ocean (1998–2023). Start and end dates of blooms with maximum PIC, colored by peak PIC concentration ( $\text{mmol.m}^{-3}$ ) in the (a) CS and (b) the BS.**

Barents Sea, which drive the bio-advection of coccolithophores. Furthermore, this evolution is influenced by sea ice coverage and uncertainties coming from the internal variability (Swart et al., 2015), which, despite its decline, still significantly impacts the surface area of the Barents Sea – exhibited an unprecedented bloom in 2023, both in intensity and spatial coverage. The persistence of favourable SSTs within the 6–16°C range and PAR, coupled with a stable water column and shallow MLDs, sustained intense bloom conditions over three months. This intensification is consistent with long-term Atlantification trends (Oziel et al., 2020; Neukermans et al., 2018), a northward migration of the polar front (Fig. A7), and haline-driven stratification (Fig. A11). The Barents bloom peaked at  $16.5 \text{ mmol.m}^{-3}$ , more than five times the 1998–2020 mean, confirming the development of blooms in high-latitude regions (Hutchins and Tagliabue, 2024) and the poleward shift of temperate phytoplankton in the Barents Sea (Neukermans et al., 2018). In addition, ecosystem responses to these changes in species distributions may be contrasted by local adaptation plans and policies (Smale et al., 2019; Smith et al., 2023).

Even if some shifts are underway, our results on phenology align with previous findings in terms of timing of the onset and bloom duration (Hopkins et al., 2015) and of increasing intensity (Rivero-Calle et al., 2015). These shifts – These contrasting responses illustrate the sensitivity of coccolithophore dynamics to both short-term (MHWs) and long-term (warming, stratification) environmental changes. The observed phenology aligns with previous phenological studies (Hopkins et al., 2015) but suggests a change since 2021, with poleward shifts in bloom intensity and extent potentially indicative of a regime transition. However,

the weak correlation between the polar front and leading-edge bloom extent and the strong correlation between SST anomaly and bloom surface extent (Table A1) suggest that while Atlantification supports expansion, MHWs are also important in reaching thermal thresholds for bloom development (Table A1). These changes need further confirmation, particularly with additional data from diverse regions ~~in the middle of the favorable region but~~ undergoing similar MHWs (e.g. North Sea) ~~and~~ combine, compare these results with numerical simulations to accurately quantify the contributions of the respective processes, both in terms of intensity and temporal variability.

310

Nevertheless, several limitations must be acknowledged. First, our estimates ~~may be lower of bloom spatial extent may be underestimated~~ due to the spatial averaging inherent in satellite observations and due to the cloud cover at high latitudes; ~~future studies should~~. Future studies could explore the use of more precise spatial masking techniques to address this or rely on potentially improved retrieval of PIC from hyperspectral ocean-colour sensors such as PACE (Werdell et al., 2019), ~~the recently~~ 315 ~~launched Plankton, Aerosols, Clouds and Ecosystems (PACE) mission (Werdell et al., 2019).~~

Our analysis was limited to surface ocean PIC concentration, detectable from ocean colour satellites. The lack of ~~vertical observational data, due to limited in situ measurements, vertically resolved observational data~~ constrains our ability to capture the vertical distribution and ~~intensity~~ PIC standing stock of these blooms. This limitation may be overcome by applying statistical ~~relationship~~ relationships extrapolating surface observations vertically (Baleh et al., 2018) (e.g. Balch et al., 2018).

320

~~This change of ecological niches is not unique to~~ Coccolithophores, like other calcifying organisms, are sensitive to ocean acidification, potentially reducing their ability to produce coccoliths. Polar regions, subject to increased ocean acidification (Gattuso and Hansson, 2011), may become less favorable for these organisms in the long-term (Terhaar et al., 2020). Additionally, the evolution of water column stratification plays a key role in promoting blooms with a clear signal in the North Atlantic which 325 ~~in fine may alter the regional carbon cycle. These dynamics, including the vertical variation of the summertime mixed-layer depth (Sallée et al., 2021), may reduce both light and nutrient availability, and also have implications for carbon export, a critical function of calcifying species. Knowing the impact of these blooms on the regional ocean carbon cycle, there is a clear interest in knowing the future evolution and implication as these weakening of the ocean carbon sink may compound with decline related to MHW events (Müller et al., 2025).~~

330

~~The changes observed in~~ 2023 ~~but reflects~~ and reaching exceptional level are an extreme signature of multi-annual variability superimposed on long-term trends. ~~Over the past two to three years, a notable shift in bloom phenology has emerged, with trailing-edge blooms occurring later in the year, particularly in autumn, a period traditionally considered less favourable for such events (return of the westerly winds associated with a southward shift of the storm-track). In contrast, bloom dynamics at the leading edge show high interannual variability with less influence on the timing, largely due to the limiting influence of PAR at~~ 335 ~~these latitudes. However, rising temperatures in the Barents Sea, which is warming faster than other basins (Rantanen et al., 2022), have led to blooms of exceptionally high intensity. These observations underscore the critical~~ There is a need to disentangle the contributions of internal climate system variability, such as decadal variability, from the impacts of anthropogenic climate change~~and~~. This will increase our capacity to assess extreme but plausible events such as the record SSTs in 2023-2024

(Terhaar et al., 2025) and anticipate their consequences. Advancing our understanding of these processes requires leveraging 340 recent advances in attribution science (Stott et al., 2016; Ribes et al., 2020; Faranda et al., 2024), which have predominantly focused on terrestrial and atmospheric systems and create similar. Similar services for oceans, incorporating biogeochemical components, could be created. This effort must be supported by the development of integrated, could be developed by considering a combination of multi-scale observation networks capable of providing the initial conditions needed to better understand processes, and enhanced modelling frameworks that capture subsurface dynamics and multi-stressor interactions 345 to anticipate future changes, and inform adaptive strategies for marine ecosystems. Such a perspective will also need to address inter-species competition, especially as changes in MLD and stratification create new subsurface conditions that could alter both predator-prey dynamics and grazing pressures (Arteaga et al., 2020). (Gregg and Casey, 2007; Nissen et al., 2018; Krumhardt et al., 2019)

~

This study reaffirms the poleward expansion of temperate phytoplankton communities and highlights the emergence of new 350 ecological hotspots in high-latitude regions (Hutchins and Tagliabue, 2024) and the dynamic of the calcifying communities intrusion in the Barents Sea (Neukermans et al., 2018). These shifts, while globally evident, impact regional biogeochemical cycles and food web dynamics. In addition, ecosystem responses to these changes in species distributions may be contrasted by local adaptation plans and policies (Smale et al., 2019; Smith et al., 2023). Predatory species, in particular, may face challenges in tracking these changing patterns, potentially disturbing trophic interactions and ecosystem functioning (Cyr et al., 2024) 355 even if this redistribution may be vertically uneven (Santana-Falcón and Séférian, 2022; Fredston et al., 2023). Nevertheless, several local and regional physical constraints could modulate these broader trends. Coccolithophores, like other calcifying organisms, are sensitive to ocean acidification, which may reduce their ability to produce coccoliths. Polar regions, subject to increased ocean acidification, may become less favorable for these organisms in the long term *in fine* altering the regional carbon cycle. Additionally, the evolution of water column stratification plays a key role. In trailing regions like the Celtic Sea, 360 increased stratification driven by thermodynamic factors is evident, whereas the Barents Sea exhibits a contrasting trend toward destratification, a process that is counter-intuitive with the warming and freshening of these waters (Oziel et al., 2017). These dynamics, including the vertical evolution of the summertime mixed-layer depth, which may reduce both light and nutrient availability (Sallée et al., 2021), also have profound implications for carbon sequestration, a critical function of calcifying species. The observed changes in bloom duration and intensity are of particular concern: the Celtic Sea's reduced intensity 365 coupled with prolonged blooms period could signal shifts in nutrient availability, light conditions, or grazing pressures, while the Barents Sea's historical increases in bloom intensity may reflect enhanced nutrient inputs, favorable light conditions, and prolonged ice-free seasons driven by Arctic warming. Understanding the long-term consequences of these changes under different emission scenarios is particularly urgent, given the identification of the Barents Sea and its diminishing sea ice as a tipping point in the Earth system (Wunderling et al., 2024).

370 These results underscore the importance of continuous monitoring and multi-scale modeling to capture the complex interplay of physical, chemical, and biological factors driving phytoplankton species composition and phenology. Further research integrating high-resolution satellite data and in situ observations is critical to predict the ecological and biogeochemical impacts of these phenological shifts under future climate scenarios. In summary, this work highlights the need for a nuanced perspective

375 on the future of phytoplankton communities in a rapidly changing ocean. While high-latitude regions may offer temporary refuge for eoccolithophores, the combined impacts of acidification, stratification changes, and ecosystem restructuring underscore the complexity of these responses. Long-term, interdisciplinary studies will be crucial to projecting the trajectory of these ecosystems and ensuring sustainable management of the services they provide under shifting environmental baselines.

380 *Data availability.* OSTIA SST data are publicly available for download from the UK Met Office dedicated website: <https://ghrsst-pp.metoffice.gov.uk/ostia-website/index.html>. Ocean color data are publicly available for download from the ACRI-ST website : <https://hermes.acri.fr>. Mixed layer depth data are publicly available on the CMEMS website : [https://data.marine.copernicus.eu/product/GLOBAL\\_MULTIYEAR\\_PHY\\_001\\_030](https://data.marine.copernicus.eu/product/GLOBAL_MULTIYEAR_PHY_001_030)/description.

## Appendix A: Appendix

### A1 Data and Methods

#### A1.1 Study sites

385 The 2023 MHW in the North Atlantic, unprecedented in its extent and intensity, provides a unique opportunity to study the resilience and adaptation of phytoplankton, ~~, including species, including EG. huxleyi~~, to extreme temperatures. In the North Atlantic, *EG. huxleyi* typically blooms annually in regions situated between the continental shelf of Western Europe ([Bay of Biscay](#)[Celtic Sea](#)) and an Arctic shelf Sea (Barents Sea), respectively representing the trailing and leading edges of the bloom distribution (Winter et al., 2014; Neukermans et al., 2018).~~To assess the impact of the 2023 MHW on *E. huxleyi* blooms, we focused on two regions situated at the northern and southern limits : To assess the impact of the 2023 MHW on *E. huxleyi*, we sampled two regions within its North Atlantic distribution:~~

390

~~The~~ Celtic Sea [14°E - 9°E / 49.7°N - 56°N] : ~~A region at the trailing edge, is a region~~ where blooms occur annually and historical marine ~~heatwaves~~[heat waves](#) have resulted in temperature anomalies of up to +5°C in June 2023 (Berthou et al., 395 2024).

~~The~~ Barents Sea [18°W - 60°W / 68°N - 80°N] : ~~A region at the leading edge, is a region~~ experiencing rapid warming and sea-ice loss due to Arctic amplification and "~~atlantification~~[Atlantification](#)" of its water ([Oziel et al., 2020](#); [He et al., 2024](#)).

400 ~~masses~~ ([Oziel et al., 2020](#); [Rantanen et al., 2022](#); [He et al., 2024](#)). Within these study sites, a bathymetry mask has been applied to limit turbid waters caused by resuspended bottom sediments and input from rivers, which create false-positive PIC signals. The bathymetric limits are respectively -150 m and -100 m for the Celtic Sea and the Barents Sea and derived from the ETOPO [2022](#) global relief model at 60 arc-second resolution (MacFerrin et al., 2024).

#### A1.2 Satellite data

##### ~~To assess ocean color anomalies~~

~~To assess anomalies in *G. huxleyi* bloom phenology and spatial extent~~, we used both the daily and the weekly-merged L3 405 multi-sensor PIC ~~product~~[products](#), derived from MERIS, MODIS, SeaWiFS, VIIRS, and OLCI, providing a 1/24° spatial resolution for 1997-2024 from the GlobColour project (<https://hermes.acri.fr/>). NASA's standard PIC algorithm (Balch et al., 2005; Gordon and Du, 2001) was used, based on remote sensing reflectance in either two or three bands in the visible and the near-infrared domain (Balch and Mitchell, 2023). Ocean colour ~~Observations~~[observations](#) are limited by the presence of clouds (predominant at high latitudes) which motivate the choice of using weekly-merged rather than daily products for the 410 climatological comparison. To construct a reliable climatology, we employed a 20-year archive (1998-2018), following ~~the approach of~~ Cael et al. (2023) who demonstrated that climate change indicators can be derived from ocean color data within a shorter time period than the 30-year WMO recommendation. Daily (~~resp.~~[- weekly](#)) anomalies were calculated by comparing daily (~~resp.~~[- weekly](#)) PIC data to the corresponding constructed seasonal climatology. ~~For PAR, only weekly-merged L3~~

multi-sensor PAR products are used, derived from MERIS, MODIS, SeaWiFS, VIIRS, and OLCI, providing a 1/24° spatial

415 resolution for 1997-2024 from the GlobColour project (<https://hermes.acri.fr/>).

For ~~SSTs~~SST, we used, as a reference climatology, the ESA-CCI level 4 Climate Data Record version 3 (CDR, Embury et al., 2024), which offers a daily and globally consistent record at 0.05° spatial resolution. The daily climatology over the 1991-2020 period is computed with a 5-day moving average. To derive the daily anomalies we compared the daily CDR data 420 to the Operational Sea surface Temperature and sea Ice Analysis (OSTIA) L4 analysis data (Donlon et al., 2012). The SST product is released on a daily basis in a regular latitude-longitude grid with a 0.05° spatial resolution. Marine heatwaves were identified following (Hobday et al., 2016) by comparing daily SSTs with a seasonally varying threshold defined as the local 90th percentile of a 30-year climatology. Periods of at least five consecutive days above this threshold were classified as marine heatwaves.

425

In the Barents Sea, ~~increased bloom frequency and intensity are driven by bio-advection and atlantification (Oziel et al., 2020)~~  
~~A proxy for atlantification is previous studies have shown that~~ the polar front, ~~which separates~~ separating Atlantic and Arctic waters. ~~We~~ water masses, acts as a physical barrier to coccolithophore bloom expansion (Neukermans et al., 2018; Oziel et al., 2020). We therefore computed the Barents Sea polar front position using a local variance filter applied to March-April OSTIA SSTs 430 with a window size of 7x7 pixels (Neukermans et al., 2018). We, first, computed the monthly average from the daily OSTIA archive. Polar Front Waters were ~~, then, defined as~~ then defined as waters having SSTs between the ~~16<sup>th</sup> and 84<sup>th</sup>~~ 16th and 84th percentiles (Oziel et al., 2016). The ~~evolution~~ shifting position of the polar front since 1998 is shown in Fig. ~~AA6 & A7~~.

#### ~~Mixed layer depth (MLD)~~

### **A1.3 Ocean stratification data**

435 MLD data were obtained from the daily GLORYS12 Version 1 reanalysis, which provides a daily and global record from 1993 to 2024 at 1/12° spatial resolution (Jean-Michel et al., 2021). ~~To evaluate the vertical temperature and the stratification, Institute of Atmospheric Physics (IAP) observation-based temperature/salinity fields at 1°x1° horizontal resolution and 41 vertical levels from 1-2000m and a monthly resolution from January 1940 to September 2023 were used. The product is described by (Cheng and Zhu, 2016; Cheng et al., 2017).~~

440 Based on this dataset, we define the upper 200-m stratification as the squared buoyancy frequency computed from the density gradient over the top 200-m layer:

$$N^2 = -\frac{g}{\rho} \frac{\partial \sigma_0}{\partial z} \Big|_{0 \geq z \geq 200}, \quad (A1)$$

where  $\sigma_0$  is potential density referenced to the surface, and  $g$  is the gravitational acceleration. The squared buoyancy frequency,  $N^2$  expressed in  $s^{-2}$ .

445

The stratification can be expressed, to a first, approximation, as a linear combination of distinct temperature and salinity contributions (Gill and Niller, 1973):

$$N^2 = N_T^2 + N_S^2, \text{ with } N_S^2 = -g\beta \frac{\partial S}{\partial z} \Big|_{0 \geq z \geq 200} \text{ and } N_T^2 = g\alpha \frac{\partial T}{\partial z} \Big|_{0 \geq z \geq 200}, \quad (\text{A2})$$

where  $\beta$  is the haline contraction coefficient and  $\alpha$  is the thermal expansion coefficient.

#### 450 A1.4 Bloom detection and phenology

To assess ~~coccolithophore~~ *G. huxleyi* bloom phenology, we applied the methods of Hopkins et al. (2015) on the L3 daily multi-sensor PIC product (Sect. A1.2). This allows us to estimate bloom start and end dates, maximum concentration, and extent knowing the limitations of such data at high latitudes. This method is based on the analysis of the temporal evolution of the PIC concentration over the study site and the identification of both a local minimum before and after the detected peak of the

455 bloom.

The ~~analysis of environmental conditions driving the onset of blooms is based on two essential conditions (a relatively warm and stratified upper ocean):~~

$MLD < 40 - 50\text{m}$  and  $SST \in [6 - 16^\circ\text{C}]$

The surface extent computation relies on the number of relevant pixel areas detected with a PIC concentration greater than a region-based threshold (defined on daily products) applied to the weekly-merged L3 products. The threshold is computed based on the 1998-2018 climatology and determined as the PIC concentration on the climatological bloom start date, serving as a baseline for identifying significant anomalies. The respective values for CS and BS are  $0.06 \text{ mmol.m}^{-3}$  and  $0.1 \text{ mmol.m}^{-3}$ . The study sites are located in mid- and high-latitudes, the surface extent must take into account the surface spherical deformation, defined as follows:

$$465 \quad S = \sum s_i \text{ with } s_i = 110.574 * \text{latitude} * 111.320 * \text{longitude} * \cos(\text{latitude}) \quad (\text{A3})$$

Based on a global compilation of in situ measurements of coccolithophore species abundance and diversity (O'Brien et al., 2013), the realized ecological niche of *G. huxleyi* (i.e. the environmental conditions under which it can be observed) has been characterized (O'Brien, 2015). Out of seven environmental variables considered, O'Brien et al. (2016) showed that SST, PAR, and MLD were the most important variables influencing coccolithophore diversity. For *G. huxleyi*, the optimal SST range is situated between 6 and  $16^\circ\text{C}$ , optimal PAR between 35 and  $42 \text{ Einstein.m}^{-2}.\text{day}^{-1}$ , and optimal MLD between 20 and 30 m.

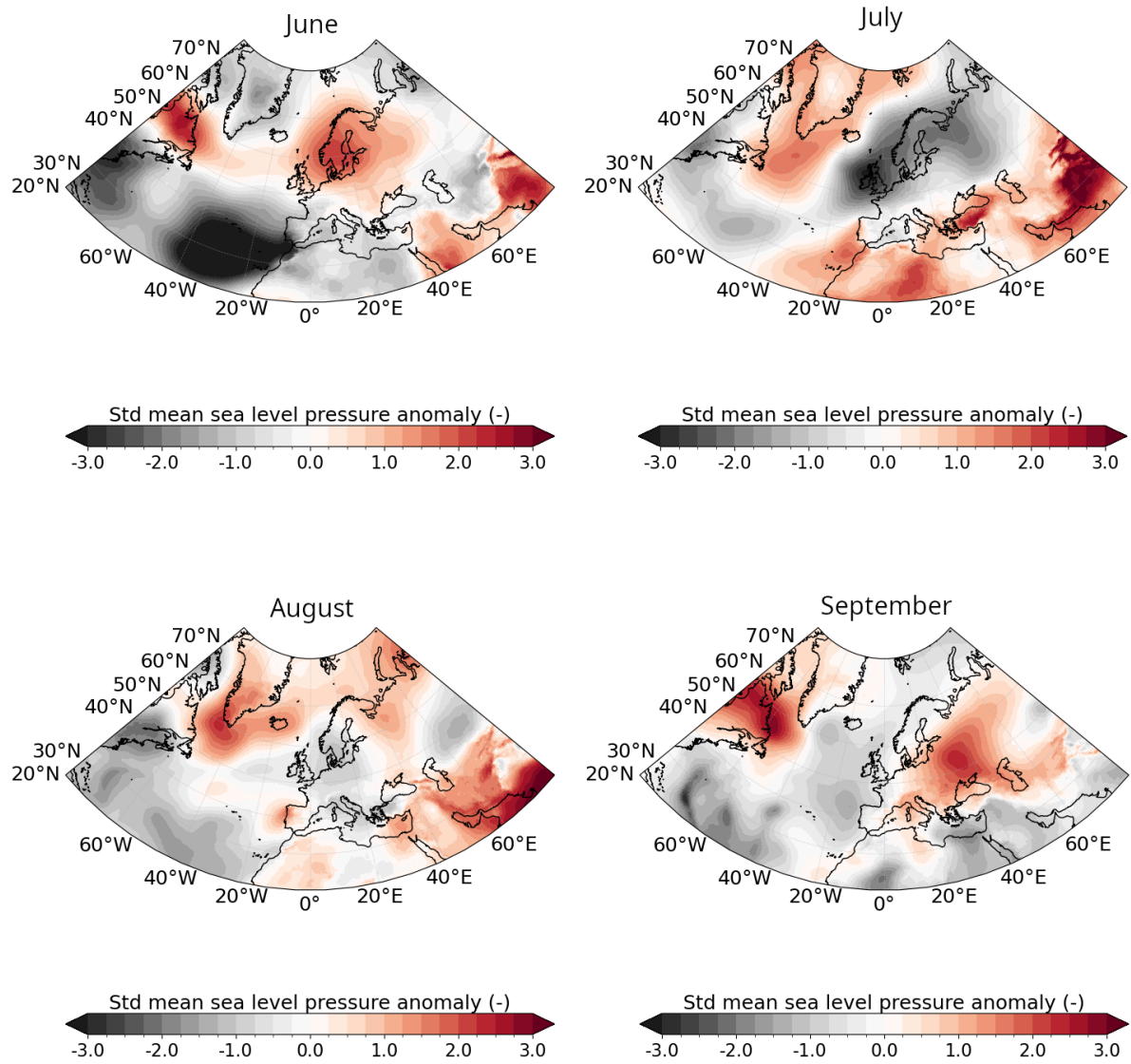


**Figure A1. Seasonal evolution of daily PIC concentration in the Celtic Sea and Barents Sea. Daily PIC concentrations ( $\text{mmol m}^{-3}$ ) averaged over 5-year Ocean-atmosphere conditions in June-July-August-September 2023. Standardised monthly anomalies from ERA5 in 2023 compared to the 1991-2020 climatological period and smoothed using a LOWESS regression for mean sea level pressure.**

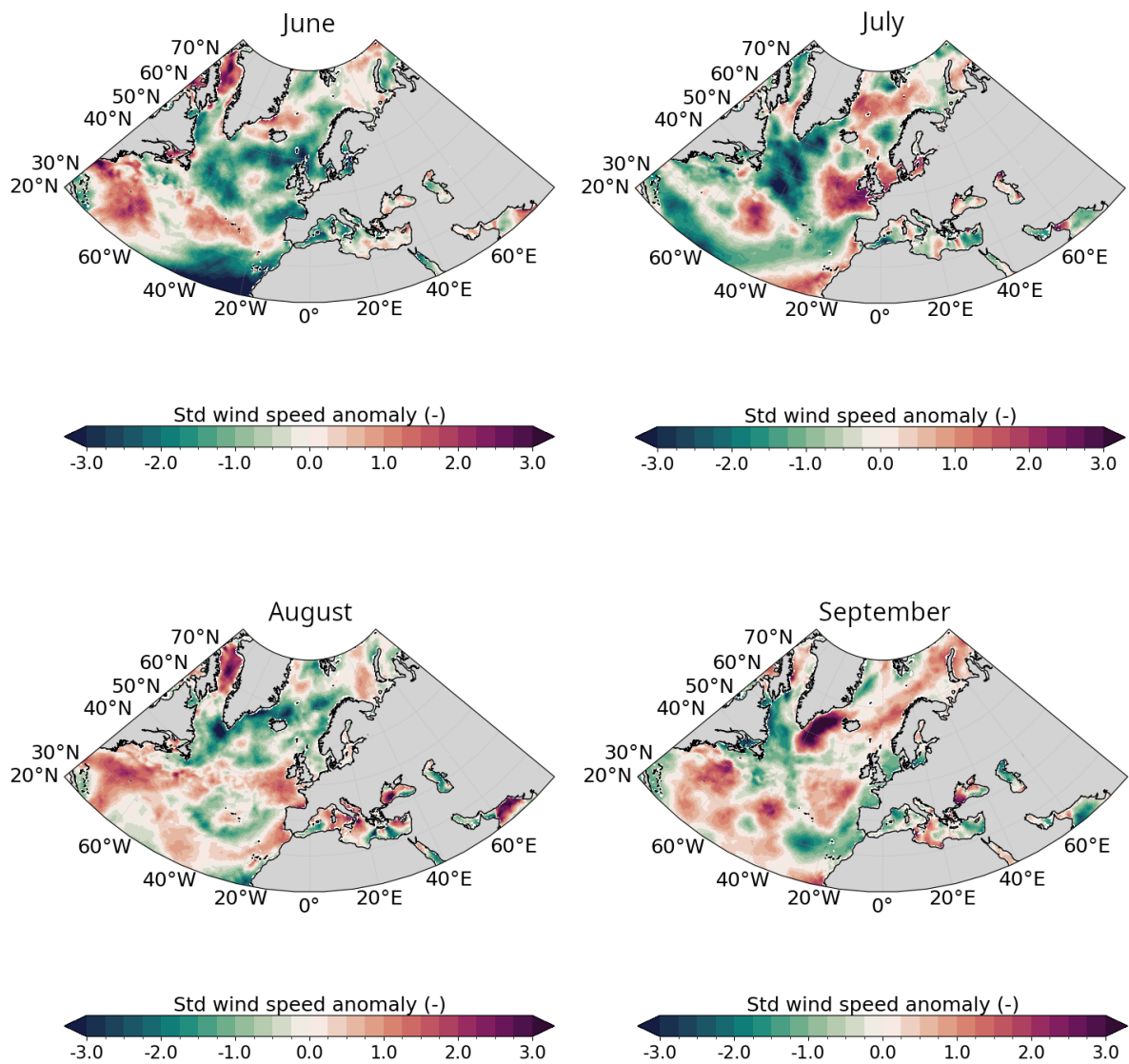


**Figure A2.** Same as Fig.A1 for 10-m wind speed.

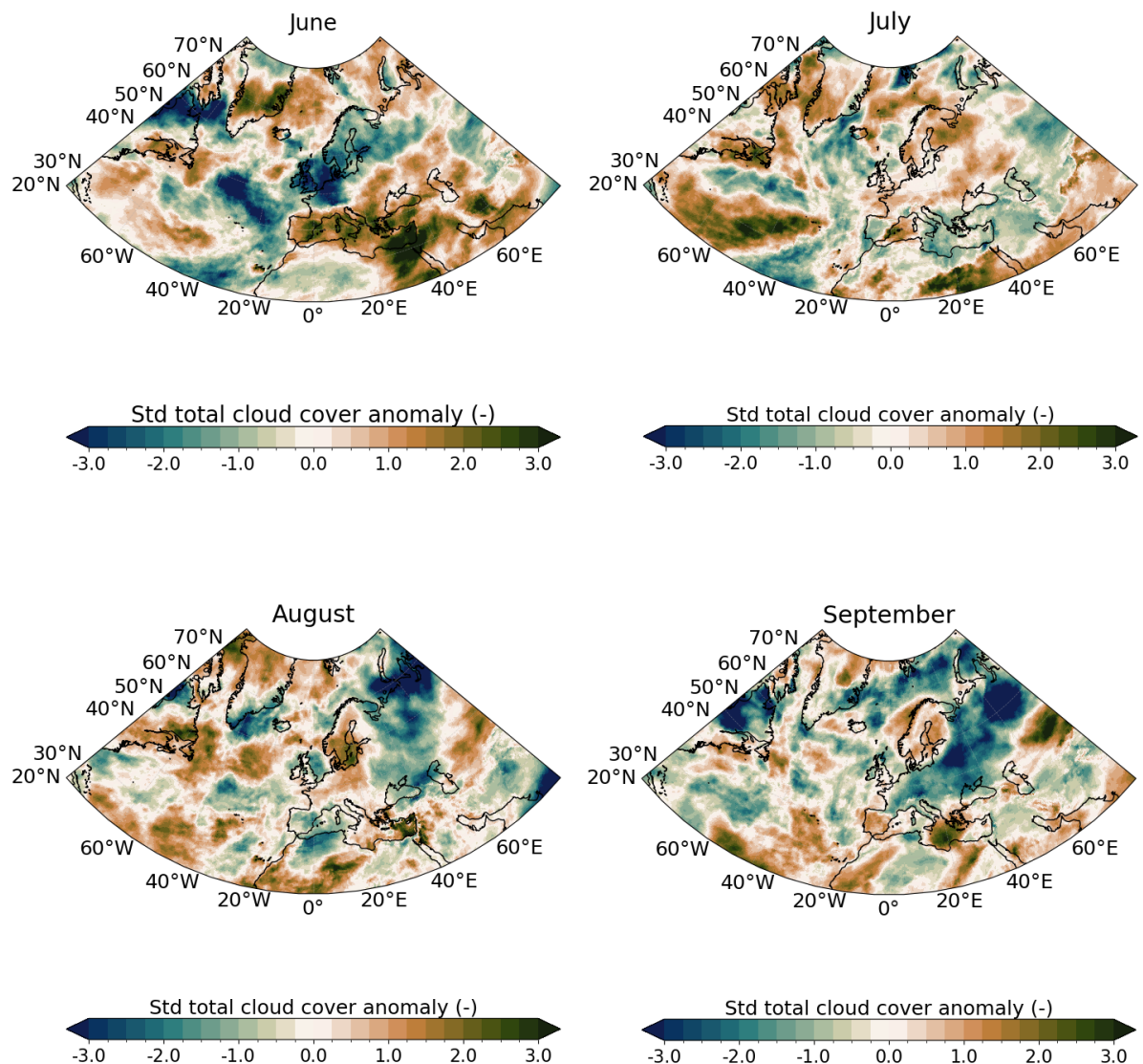


**Figure A3.** Same as Fig.A1 for total cloud cover.

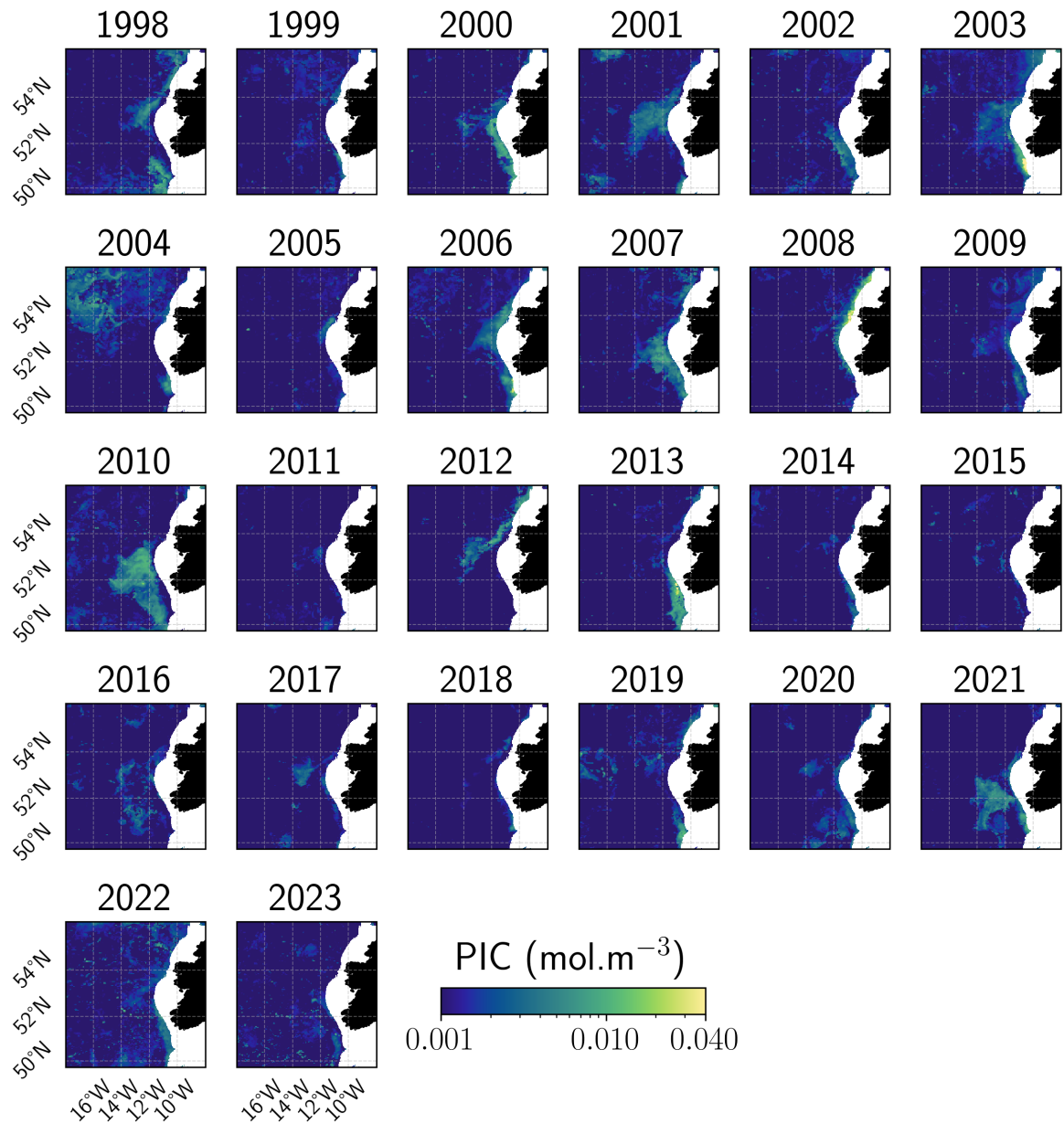
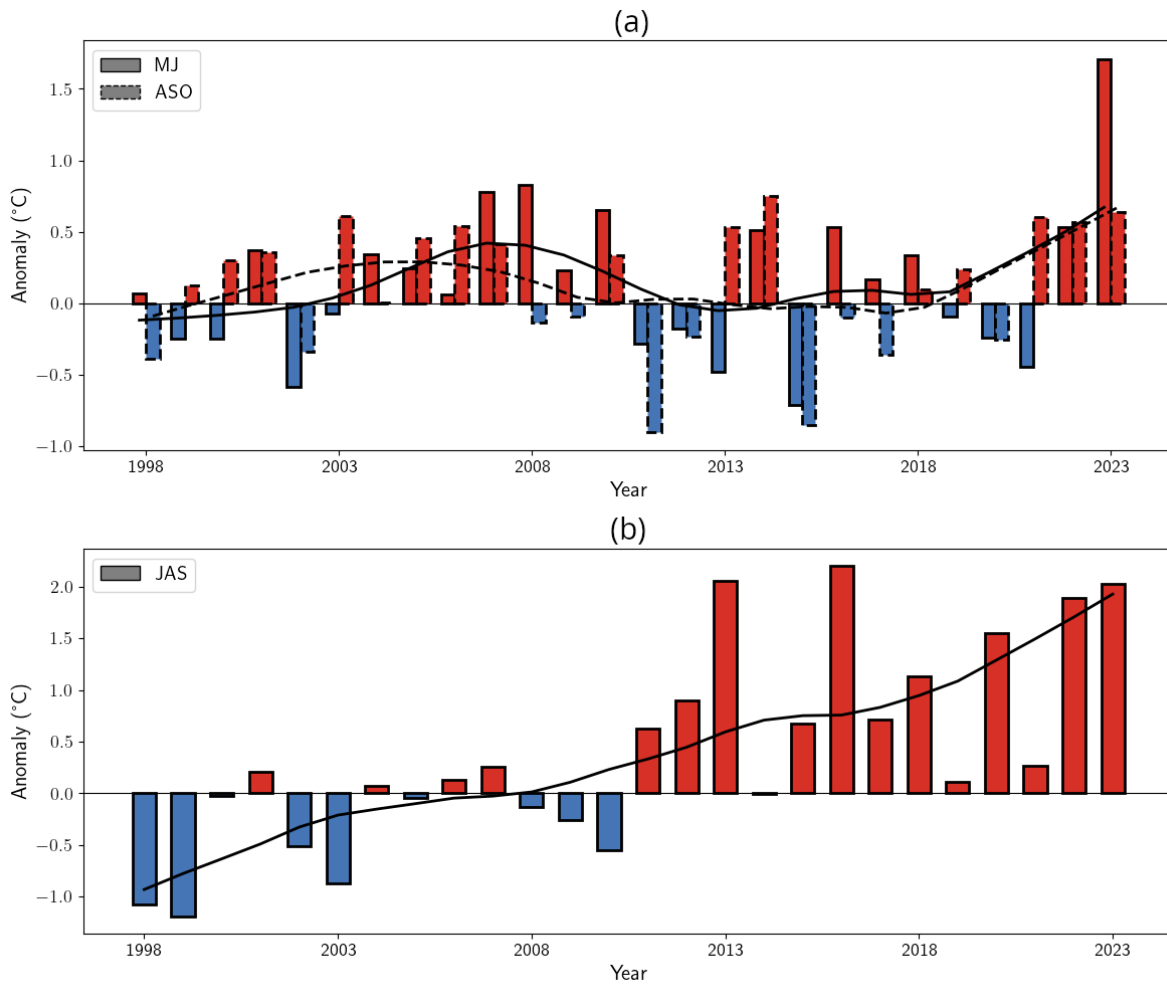


**Figure A4. Summer maximum PIC concentration in the Celtic Sea.** Annual evolution of the remotely-sensed summer maximum PIC concentration. White areas defined coastal zones where the bathymetry is higher than -150m.



**Summer maximum PIC concentration in the Celtic Sea.** Annual evolution of The line indicated the remotely-sensed summer maximum PIC concentration 10-year LOESS trend. White areas defined coastal zones where the bathymetry is higher than -150m.

**Summer maximum PIC concentration in the Celtic Sea.** Annual evolution of The line indicated the remotely-sensed summer maximum PIC concentration 10-year LOESS trend. White areas defined coastal zones where the bathymetry is higher than -150m.

**Figure A5. Long-term SST evolution in the Celtic and Barents seas.** SST anomalies for (a) the Celtic Sea (May-June in solid contour & August-September-August in dashed contour) and (b) the Barents Sea (July-August-September), computed relatively to the 1991–2020 climatological period. The year 2023 is highlighted in red. Red bars indicate positive anomalies, while blue bars denote negative anomalies.

**Summer maximum PIC concentration in the Celtic Sea.** Annual evolution of The line indicated the remotely-sensed summer maximum PIC concentration 10-year LOESS trend. White areas defined coastal zones where the bathymetry is higher than -150m.

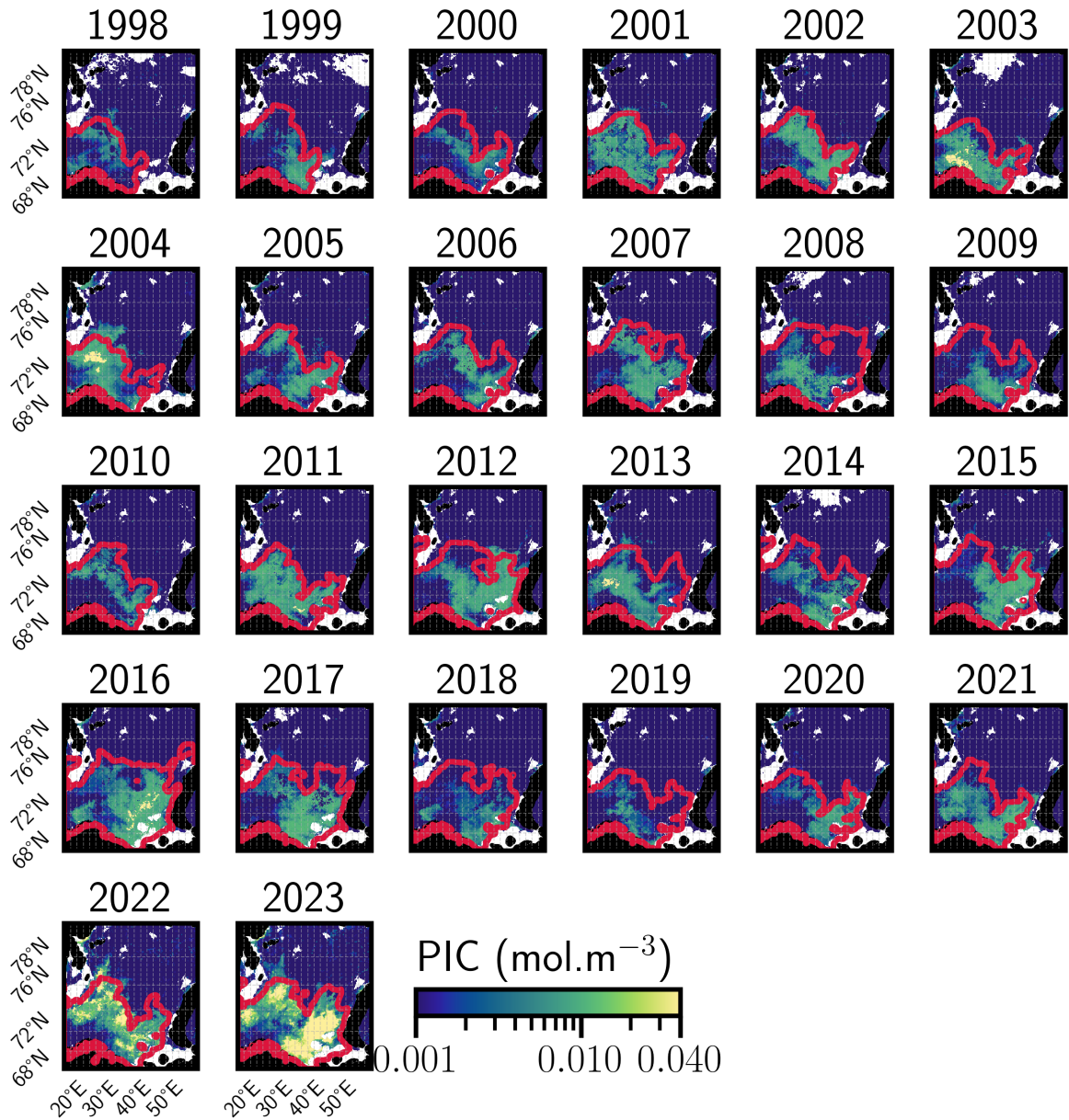


**Figure A6. Summer maximum PIC concentration in the Barents Sea.** Annual evolution of the remotely-sensed summer maximum PIC concentration and the corresponding polar front in red. The polar front is based on an analysis of the ice-free March-April SSTs. White areas defined coastal zones where the bathymetry is higher than -100m.

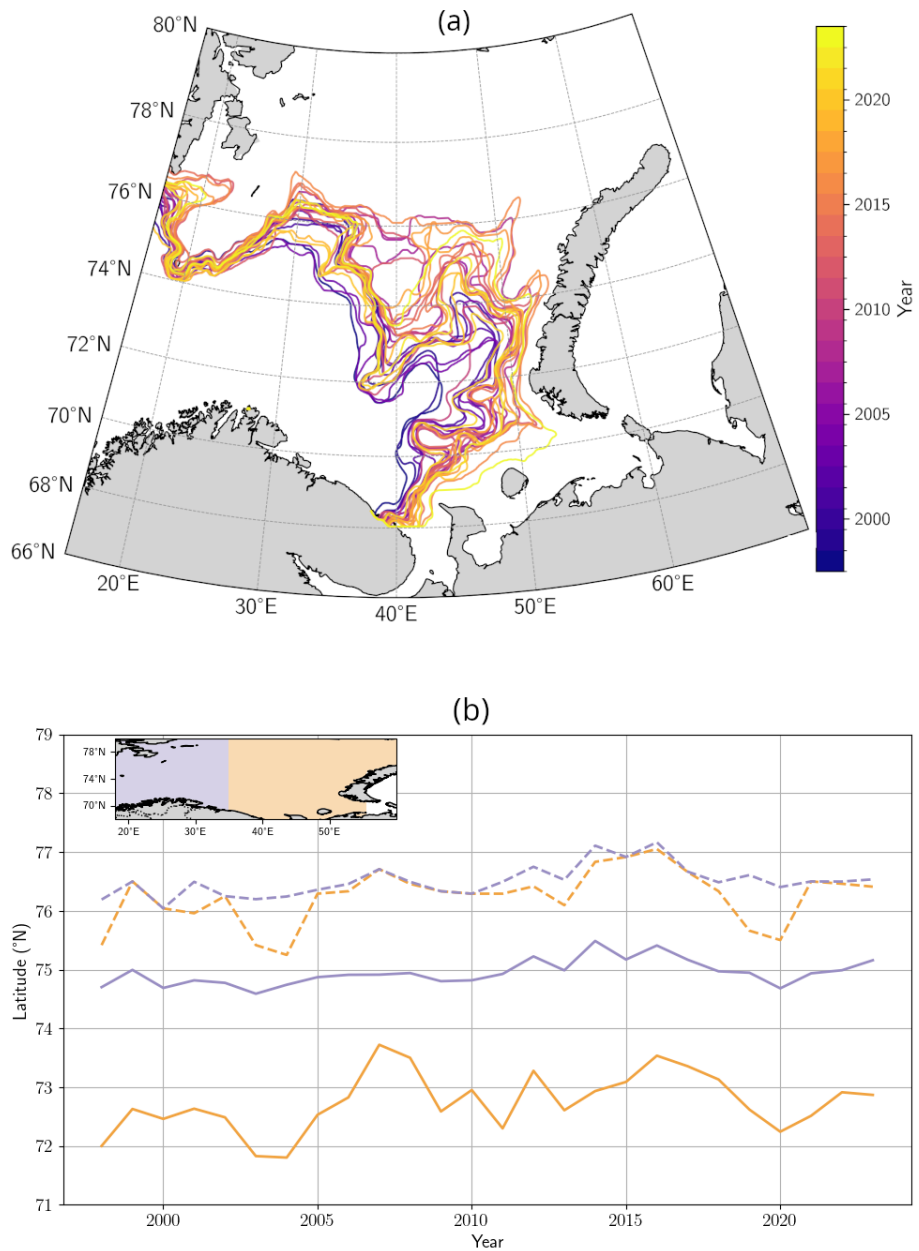


**Figure A7. Shifting position of the polar front in the Barents Sea.** (a) Position of the polar front in the Barents Sea obtained from remotely sensed SST imagery and (b) corresponding position of the polar front maximum latitude in the western (blue lines) and eastern (orange lines) basins of the Barents Sea over the period 1998-2023.

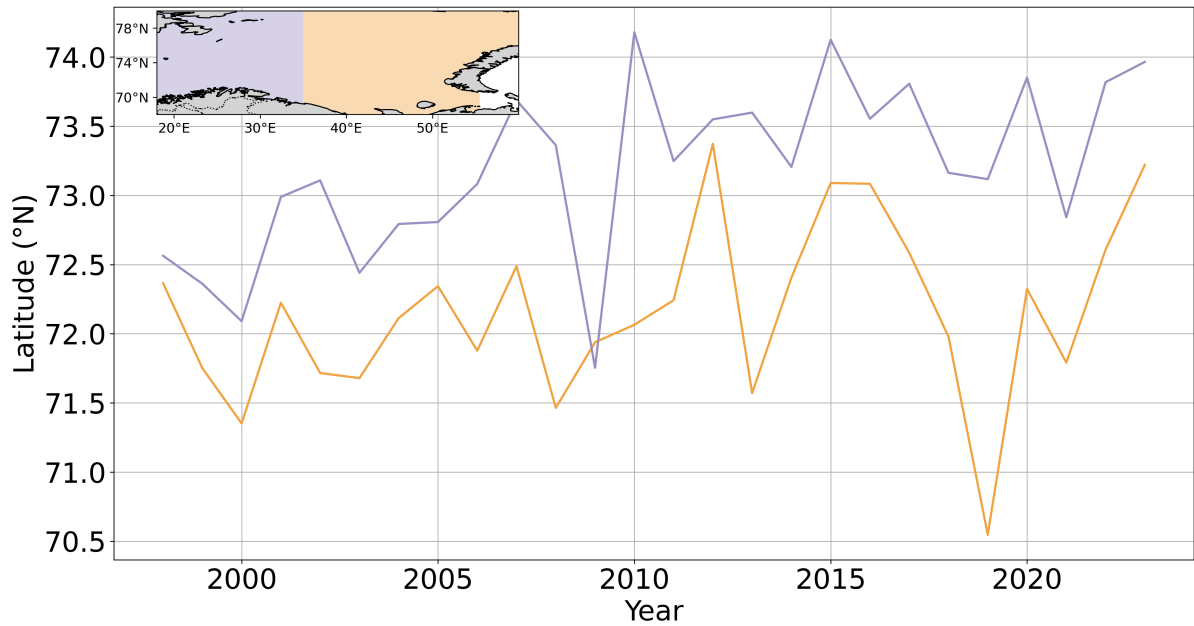


**Figure A8. Decadal evolution of summer mean PIC concentration in the Celtic Sea and Barents Sea. Barcode plots Shifting position of the leading edge of *G. huxleyi* summer blooms in the Barents Sea. Temporal evolution of the distribution mean latitude of yearly the bloom summer (June-July-August) mean PIC concentrations ( $\text{mmol m}^{-3}$ ). Colors refer to maximum extent for the corresponding decade with decadal means indicated by black dashed lines: western (blue lines) Celtic sea and eastern (orange lines) basins of the Barents Sea over the period 1998-2023.**

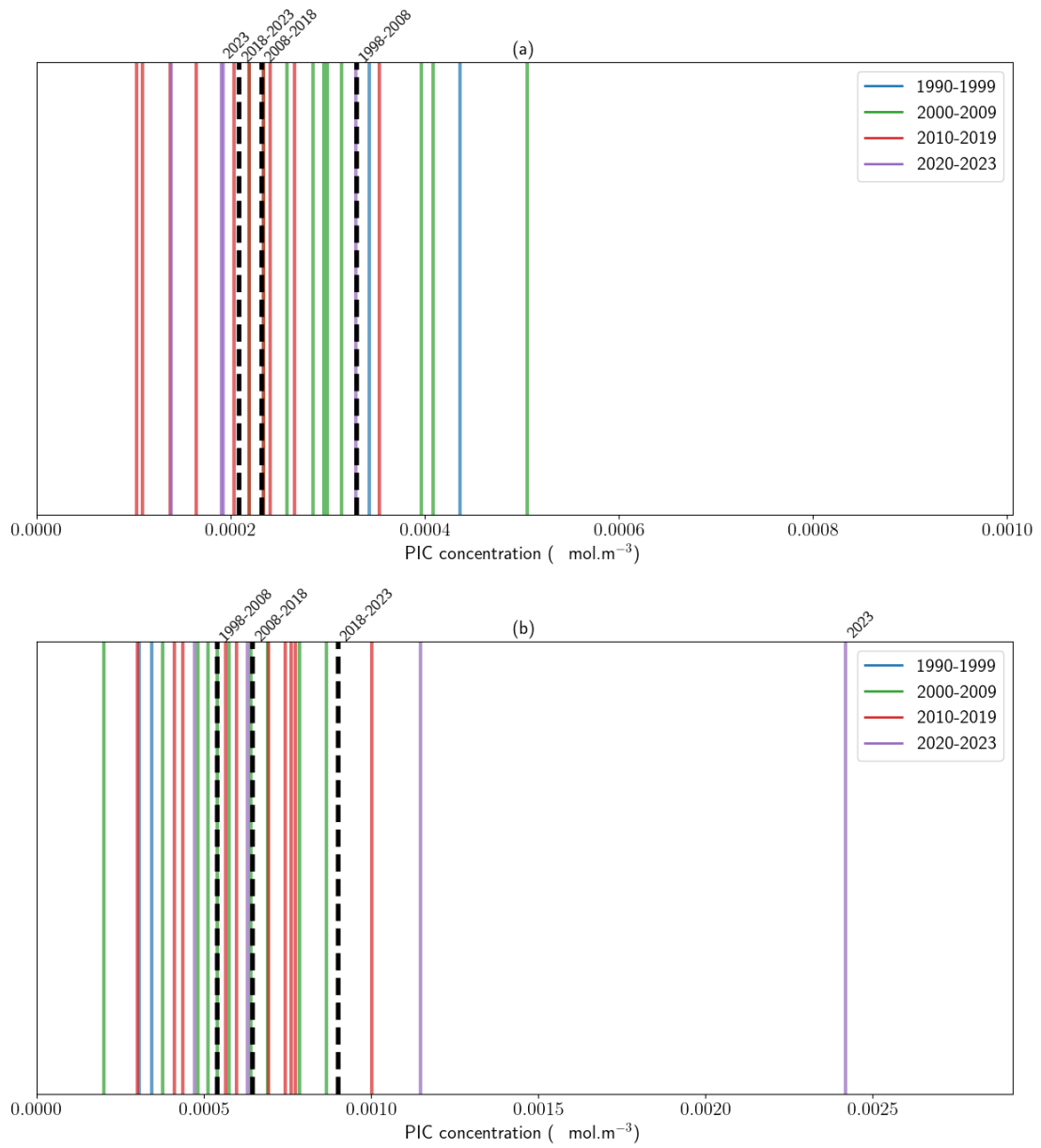


**Figure A9. Decadal evolution of summer mean PIC concentration in the Celtic Sea and Barents seas.** Barcode plots of the distribution of yearly summer (June-July-August) mean PIC concentrations ( $\text{mol} \cdot \text{m}^{-3}$ ). Colors refer to the corresponding decade with decadal means indicated by black dashed lines. (a) Celtic sea and (b) Barents Sea.

**Evolution of the standardized anomalies of summertime (July–August) SSTs and PIC over the Barents Sea.** Yearly standardised anomalies of SSTs (blue) and PIC (brown) compared to respectively the 1991–2020 and the 1998–2017 climatological period. Pearson correlation coefficient indicate the strength of correlation between the standardised anomalies and the \*\*\* refers to a  $p_{value} < 0.01$ .

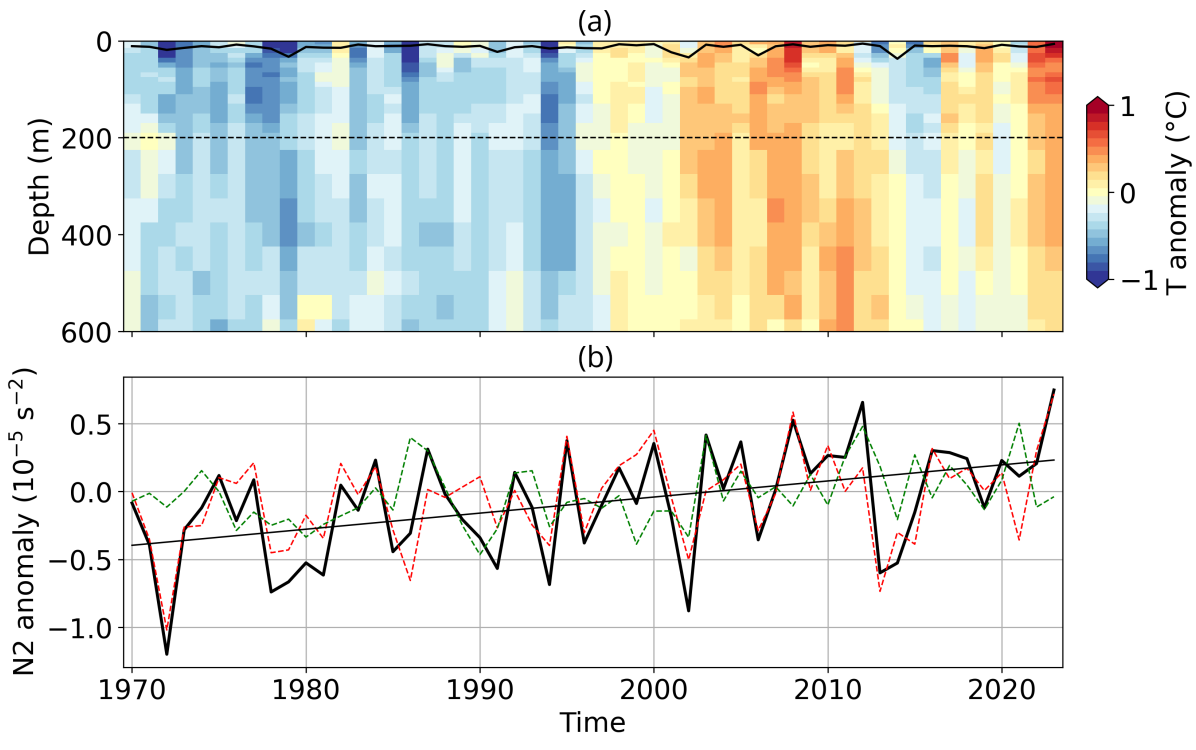


**Figure A10. Stratification conditions in the Celtic Sea.** Vertical profile of (a) May–June anomalous temperature compared to the 1991–2020 climatological mean from the IPA dataset (b) time-series of the 0–200 m stratification anomaly,  $N^2$  and temperature (red dashed) and haline contribution (green dashed) to stratification in the Celtic Sea.

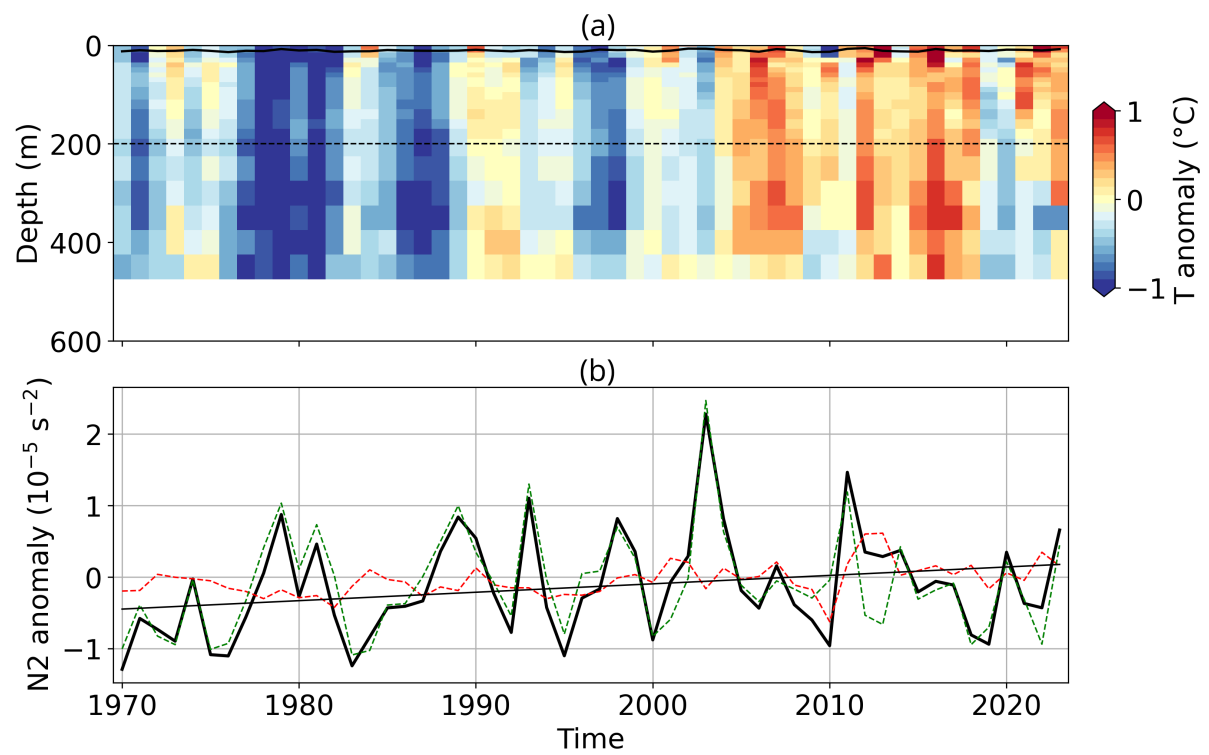


**Figure A11. Stratification conditions in the Barents Sea.** Same as Fig. A10 for the Barents Sea.

Region name		MJ SST anomaly	JAS SST anomaly
Celtic	mean surface ano	0.76***	0.98***
	max surface ano	0.70***	0.77***
Barents	mean surface ano	—	0.95***
	max surface ano	—	0.96***

**Table A1. Statistical analysis on the impact of SST on surface blooms.** Correlation coefficient between bloom surface extent anomaly and summer SST anomaly in the Barents and Celtic Seas. \*\*\* correspond to a p\_value < 0.01 (Student t-test).

*Author contributions.* TG and GN designed the study; TG conducted analysis and wrote the paper with contributions from GN. TG and GN took part in discussions and revisions of the paper.

*Competing interests.* The contact author has declared that none of the authors has any competing interests.

*Disclaimer.* TEXT

475 *Acknowledgements.* This work is a contribution to CarbOcean (European Research Council under the European Union's Horizon 2020 research and innovation programme Grant agreement No. 853516) awarded to GN. TG sincerely thanks Jean-Baptiste Sallée for many fruitful discussions on the evolution of current dynamics in the Barents Sea and for providing with stratification diagnostics. TG sincerely thanks Christophe Cassou for his mentoring and help in understanding climate internal variability.

## References

480 Ackleson, S., Balch, W., and Holligan, P.: White waters of the Gulf of Maine, *Oceanography*, 1, 18–22, 1988.

Ardyna, M., Babin, M., Gosselin, M., Devred, E., Rainville, L., and Tremblay, J.-É.: Recent Arctic Ocean sea ice loss triggers novel fall phytoplankton blooms, *Geophysical Research Letters*, 41, 6207–6212, 2014.

Arteaga, L. A. and Rousseaux, C. S.: Impact of Pacific Ocean heatwaves on phytoplankton community composition, *Communications Biology*, 6, 263, 2023.

485 Arteaga, L. A., Boss, E., Behrenfeld, M. J., Westberry, T. K., and Sarmiento, J. L.: Seasonal modulation of phytoplankton biomass in the Southern Ocean, *Nature Communications*, 11, 5364, 2020.

Árthun, M., Eldevik, T., Smedsrød, L. H., Skagseth, Ø., and Ingvaldsen, R.: Quantifying the influence of Atlantic heat on Barents Sea ice variability and retreat, *Journal of Climate*, 25, 4736–4743, 2012.

490 Balch, W., Gordon, H. R., Bowler, B., Drapeau, D., and Booth, E.: Calcium carbonate measurements in the surface global ocean based on Moderate-Resolution Imaging Spectroradiometer data, *Journal of Geophysical Research: Oceans*, 110, 2005.

Balch, W. M. and Mitchell, C.: Remote sensing algorithms for particulate inorganic carbon (PIC) and the global cycle of PIC, *Earth-Science Reviews*, 239, 104 363, 2023.

Balch, W. M., Bowler, B. C., Drapeau, D. T., Lubelczyk, L. C., and Lyczkowski, E.: Vertical distributions of coccolithophores, PIC, POC, biogenic Silica, and chlorophyll a throughout the global ocean, *Global Biogeochemical Cycles*, 32, 2–17, 2018.

495 Beaugrand, G., McQuatters-Gollop, A., Edwards, M., and Goberville, E.: Long-term responses of North Atlantic calcifying plankton to climate change, *Nature Climate Change*, 3, 263–267, 2013.

Bendif, E. M., Probert, I., Archontikis, O. A., Young, J. R., Beaufort, L., Rickaby, R. E., and Filatov, D.: Rapid diversification underlying the global dominance of a cosmopolitan phytoplankton, *The ISME Journal*, 17, 630–640, 2023.

Berthou, S., Renshaw, R., Smyth, T., Tinker, J., Grist, J. P., Wihsott, J. U., Jones, S., Inall, M., Nolan, G., Berx, B., et al.: Exceptional 500 atmospheric conditions in June 2023 generated a northwest European marine heatwave which contributed to breaking land temperature records, *Communications Earth & Environment*, 5, 287, 2024.

Burger, F. A., Terhaar, J., and Frölicher, T. L.: Compound marine heatwaves and ocean acidity extremes, *Nature communications*, 13, 4722, 2022.

Cael, B., Bisson, K., Boss, E., Dutkiewicz, S., and Henson, S.: Global climate-change trends detected in indicators of ocean ecology, *Nature*, 505 619, 551–554, 2023.

Capotondi, A., Rodrigues, R. R., Sen Gupta, A., Benthuyzen, J. A., Deser, C., Frölicher, T. L., Lovenduski, N. S., Amaya, D. J., Le Grix, N., Xu, T., et al.: A global overview of marine heatwaves in a changing climate, *Communications Earth & Environment*, 5, 701, 2024.

Chafik, L., Nilsson, J., Skagseth, Ø., and Lundberg, P.: On the flow of Atlantic water and temperature anomalies in the Nordic Seas toward the Arctic Ocean, *Journal of Geophysical Research: Oceans*, 120, 7897–7918, 2015.

510 Cheng, L. and Zhu, J.: Benefits of CMIP5 multimodel ensemble in reconstructing historical ocean subsurface temperature variations, *Journal of Climate*, 29, 5393–5416, 2016.

Cheng, L., Trenberth, K. E., Fasullo, J., Boyer, T., Abraham, J., and Zhu, J.: Improved estimates of ocean heat content from 1960 to 2015, *Science Advances*, 3, e1601 545, 2017.

Cheng, L., von Schuckmann, K., Abraham, J. P., Trenberth, K. E., Mann, M. E., Zanna, L., England, M. H., Zika, J. D., Fasullo, J. T., Yu, Y., 515 et al.: Past and future ocean warming, *Nature Reviews Earth & Environment*, 3, 776–794, 2022.

Cheung, W. W. and Frölicher, T. L.: Marine heatwaves exacerbate climate change impacts for fisheries in the northeast Pacific, *Scientific reports*, 10, 6678, 2020.

Cyr, F., Lewis, K., Bélanger, D., Regular, P., Clay, S., and Devred, E.: Physical controls and ecological implications of the timing of the spring phytoplankton bloom on the Newfoundland and Labrador shelf, *Limnology and Oceanography Letters*, 9, 191–198, 2024.

520 de Boyer Montégut, C., Madec, G., Fischer, A. S., Lazar, A., and Iudicone, D.: Mixed layer depth over the global ocean: An examination of profile data and a profile-based climatology, *Journal of Geophysical Research: Oceans*, 109, 2004.

Donlon, C. J., Martin, M., Stark, J., Roberts-Jones, J., Fiedler, E., and Wimmer, W.: The operational sea surface temperature and sea ice analysis (OSTIA) system, *Remote Sensing of Environment*, 116, 140–158, 2012.

D'Amario, B., Pérez, C., Grelaud, M., Pitta, P., Krasakopoulou, E., and Ziveri, P.: Coccolithophore community response to ocean acidification 525 and warming in the Eastern Mediterranean Sea: results from a mesocosm experiment, *Scientific reports*, 10, 12 637, 2020.

Embry, O., Merchant, C. J., Good, S. A., Rayner, N. A., Høyer, J. L., Atkinson, C., Block, T., Alerskans, E., Pearson, K. J., Worsfold, M., et al.: Satellite-based time-series of sea-surface temperature since 1980 for climate applications, *Scientific Data*, 11, 326, 2024.

England, M. H., Li, Z., Huguenin, M. F., Kiss, A. E., Sen Gupta, A., Holmes, R. M., and Rahmstorf, S.: Drivers of the extreme North Atlantic marine heatwave during 2023, *Nature*, pp. 1–8, 2025.

530 Faranda, D., Messori, G., Coppola, E., Alberti, T., Vrac, M., Pons, F., Yiou, P., Saint Lu, M., Hisi, A. N., Brockmann, P., et al.: ClimaMeter: contextualizing extreme weather in a changing climate, *Weather and Climate Dynamics*, 5, 959–983, 2024.

Fiddes, S. L., Woodhouse, M. T., Nicholls, Z., Lane, T. P., and Schofield, R.: Cloud, precipitation and radiation responses to large perturbations in global dimethyl sulfide, *Atmospheric Chemistry and Physics*, 18, 10 177–10 198, 2018.

Forster, P. M., Smith, C., Walsh, T., Lamb, W. F., Lamboll, R., Hall, B., Hauser, M., Ribes, A., Rosen, D., Gillett, N. P., et al.: Indicators 535 of Global Climate Change 2023: annual update of key indicators of the state of the climate system and human influence, *Earth System Science Data*, 16, 2625–2658, 2024.

Forster, P. M., Smith, C., Walsh, T., Lamb, W. F., Lamboll, R., Cassou, C., Hauser, M., Hausfather, Z., Lee, J.-Y., Palmer, M. D., et al.: Indicators of Global Climate Change 2024: annual update of key indicators of the state of the climate system and human influence, *Earth System Science Data Discussions*, 2025, 1–72, 2025.

540 Fredston, A. L., Cheung, W. W., Frölicher, T. L., Kitchel, Z. J., Maureaud, A. A., Thorson, J. T., Auber, A., Mérigot, B., Palacios-Abrantes, J., Palomares, M. L. D., et al.: Marine heatwaves are not a dominant driver of change in demersal fishes, *Nature*, 621, 324–329, 2023.

Gattuso, J.-P. and Hansson, L.: Ocean acidification, Oxford university press, 2011.

Gill, A. and Niller, P.: The theory of the seasonal variability in the ocean, in: *Deep Sea Research and Oceanographic Abstracts*, vol. 20, pp. 545 141–177, Elsevier, 1973.

Gordon, H. R. and Du, T.: Light scattering by nonspherical particles: application to coccoliths detached from *Emiliania huxleyi*, *Limnology and Oceanography*, 46, 1438–1454, 2001.

Gregg, W. W. and Casey, N. W.: Modeling coccolithophores in the global oceans, *Deep Sea Research Part II: Topical Studies in Oceanography*, 54, 447–477, 2007.

Guinaldo, T., Voldoire, A., Waldman, R., Saux Picart, S., and Roquet, H.: Response of the sea surface temperature to heatwaves during the 550 France 2022 meteorological summer, *Ocean Science*, 19, 629–647, 2023.

Guinaldo, T., Cassou, C., Sallée, J.-B., and Liné, A.: Internal variability effects doped by climate change drove the 2023 marine heat extreme in the North Atlantic, *Nature Communications : Earth & Environment*, 2025.

He, Y., Shu, Q., Wang, Q., Song, Z., Zhang, M., Wang, S., Zhang, L., Bi, H., Pan, R., and Qiao, F.: Arctic Amplification of marine heatwaves under global warming, *Nature Communications*, 15, 8265, 2024.

555 Hobday, A. J., Alexander, L. V., Perkins, S. E., Smale, D. A., Straub, S. C., Oliver, E. C., BenthuySEN, J. A., Burrows, M. T., Donat, M. G., Feng, M., et al.: A hierarchical approach to defining marine heatwaves, *Progress in oceanography*, 141, 227–238, 2016.

Holbrook, N. J., Sen Gupta, A., Oliver, E. C., Hobday, A. J., BenthuySEN, J. A., Scannell, H. A., Smale, D. A., and Wernberg, T.: Keeping pace with marine heatwaves, *Nature Reviews Earth & Environment*, 1, 482–493, 2020.

Hopkins, J., Henson, S. A., Painter, S. C., Tyrrell, T., and Poulton, A. J.: Phenological characteristics of global coccolithophore blooms, 560 *Global Biogeochemical Cycles*, 29, 239–253, 2015.

Hurrell, J. W., Kushnir, Y., Ottersen, G., and Visbeck, M.: An overview of the North Atlantic oscillation, *Geophysical Monograph-American Geophysical Union*, 134, 1–36, 2003.

Hutchins, D. A. and Tagliabue, A.: Feedbacks between phytoplankton and nutrient cycles in a warming ocean, *Nature Geoscience*, pp. 1–8, 2024.

565 Jean-Michel, L., Eric, G., Romain, B.-B., Gilles, G., Angélique, M., Marie, D., Clément, B., Mathieu, H., Olivier, L. G., Charly, R., et al.: The Copernicus global 1/12 oceanic and sea ice GLORYS12 reanalysis, *Frontiers in Earth Science*, 9, 698 876, 2021.

Kondrik, D., Pozdnyakov, D., and Johannessen, O.: Satellite evidence that *E. huxleyi* phytoplankton blooms weaken marine carbon sinks, *Geophysical Research Letters*, 45, 846–854, 2018.

Krumhardt, K. M., Lovenduski, N. S., Long, M. C., Lévy, M., Lindsay, K., Moore, J. K., and Nissen, C.: Coccolithophore growth and 570 calcification in an acidified ocean: Insights from community Earth system model simulations, *Journal of Advances in Modeling Earth Systems*, 11, 1418–1437, 2019.

Le Grix, N., Zscheischler, J., Rodgers, K. B., Yamaguchi, R., and Frölicher, T. L.: Hotspots and drivers of compound marine heatwaves and low net primary production extremes, *Biogeosciences*, 19, 5807–5835, 2022.

Levitus, S., Matishov, G., Seidov, D., and Smolyar, I.: Barents Sea multidecadal variability, *Geophysical Research Letters*, 36, 2009.

575 Li, Z., England, M. H., and Groeskamp, S.: Recent acceleration in global ocean heat accumulation by mode and intermediate waters, *Nature Communications*, 14, 6888, 2023.

MacFerrin, M., Amante, C., Carignan, K., Love, M., and Lim, E.: The earth topography 2022 (ETOPO 2022) global dem dataset, *Earth System Science Data Discussions*, 2024, 1–24, 2024.

Mahmood, R., von Salzen, K., Norman, A.-L., Galí, M., and Levasseur, M.: Sensitivity of Arctic sulfate aerosol and clouds to changes in 580 future surface seawater dimethylsulfide concentrations, *Atmospheric Chemistry and Physics*, 19, 6419–6435, 2019.

Malin, G., Turner, S., Liss, P., Holligan, P., and Harbour, D.: Dimethylsulphide and dimethylsulphonopropionate in the Northeast Atlantic during the summer coccolithophore bloom, *Deep Sea Research Part I: Oceanographic Research Papers*, 40, 1487–1508, 1993.

Meyer, J. and Riebesell, U.: Reviews and Syntheses: Responses of coccolithophores to ocean acidification: a meta-analysis, *Biogeosciences*, 12, 1671–1682, 2015.

585 Minière, A., von Schuckmann, K., Sallée, J.-B., and Vogt, L.: Robust acceleration of Earth system heating observed over the past six decades, *Scientific Reports*, 13, 22 975, 2023.

Moore, T. S., Dowell, M. D., and Franz, B. A.: Detection of coccolithophore blooms in ocean color satellite imagery: A generalized approach for use with multiple sensors, *Remote sensing of environment*, 117, 249–263, 2012.

Müller, J. D., Gruber, N., Schneuwly, A., Bakker, D. C., Gehlen, M., Gregor, L., Hauck, J., Landschützer, P., and McKinley, G. A.: Unexpected 590 decline in the ocean carbon sink under record-high sea surface temperatures in 2023, *Nature Climate Change*, pp. 1–8, 2025.

Neukermans, G. and Fournier, G.: Optical modeling of spectral backscattering and remote sensing reflectance from *Emiliania huxleyi* blooms, *Frontiers in Marine Science*, 5, 146, 2018.

Neukermans, G., Oziel, L., and Babin, M.: Increased intrusion of warming Atlantic water leads to rapid expansion of temperate phytoplankton in the Arctic, *Global Change Biology*, 24, 2545–2553, 2018.

595 Neukermans, G., Bach, L., Butterley, A., Sun, Q., Claustre, H., and Fournier, G.: Quantitative and mechanistic understanding of the open ocean carbonate pump-perspectives for remote sensing and autonomous in situ observation, *Earth-Science Reviews*, 239, 104 359, 2023.

Nissen, C., Vogt, M., Münnich, M., Gruber, N., and Haumann, F. A.: Factors controlling coccolithophore biogeography in the Southern Ocean, *Biogeosciences*, 15, 6997–7024, 2018.

O'Brien, C. J., Peloquin, J. A., Vogt, M., Heinle, M., Gruber, N., Ajani, P., Andrleit, H., Arístegui, J., Beaufort, L., Estrada, M., et al.: 600 Global marine plankton functional type biomass distributions: coccolithophores, *Earth System Science Data*, 5, 259–276, 2013.

Oliver, E. C., Donat, M. G., Burrows, M. T., Moore, P. J., Smale, D. A., Alexander, L. V., BenthuySEN, J. A., Feng, M., Sen Gupta, A., Hobday, A. J., et al.: Longer and more frequent marine heatwaves over the past century, *Nature communications*, 9, 1–12, 2018.

Oliver, E. C., BenthuySEN, J. A., Darmaraki, S., Donat, M. G., Hobday, A. J., Holbrook, N. J., Schlegel, R. W., and Sen Gupta, A.: Marine heatwaves, *Annual review of marine science*, 13, 313–342, 2021.

605 Oziel, L., Sirven, J., and Gascard, J.-C.: The Barents Sea frontal zones and water masses variability (1980–2011), *Ocean Science*, 12, 169–184, 2016.

Oziel, L., Neukermans, G., Ardyna, M., Lancelot, C., Tison, J.-L., Wassmann, P., Sirven, J., Ruiz-Pino, D., and Gascard, J.-C.: Role for A tlantic inflows and sea ice loss on shifting phytoplankton blooms in the B arents S ea, *Journal of Geophysical Research: Oceans*, 122, 5121–5139, 2017.

610 Oziel, L., Baudena, A., Ardyna, M., Massicotte, P., Randelhoff, A., Sallée, J.-B., Ingvaldsen, R. B., Devred, E., and Babin, M.: Faster Atlantic currents drive poleward expansion of temperate phytoplankton in the Arctic Ocean, *Nature Communications*, 11, 1705, 2020.

O'Brien, C. J.: Global-scale distributions of marine haptophyte phytoplankton, Phd thesis, ETH Zurich, available at <https://www.research-collection.ethz.ch/bitstream/handle/20.500.11850/155234/eth-48069-01.pdf?sequence=1>, 2015.

O'Brien, C. J., Vogt, M., and Gruber, N.: Global coccolithophore diversity: Drivers and future change, *Progress in Oceanography*, 140, 27–42, 615 2016.

Poulton, A. J., Adey, T. R., Balch, W. M., and Holligan, P. M.: Relating coccolithophore calcification rates to phytoplankton community dynamics: Regional differences and implications for carbon export, *Deep Sea Research Part II: Topical Studies in Oceanography*, 54, 538–557, 2007.

Rantanen, M., Karpechko, A. Y., Lipponen, A., Nordling, K., Hyvärinen, O., Ruosteenoja, K., Vihma, T., and Laaksonen, A.: The Arctic has 620 warmed nearly four times faster than the globe since 1979, *Communications earth & environment*, 3, 168, 2022.

Ribes, A., Thao, S., and Cattiaux, J.: Describing the relationship between a weather event and climate change: a new statistical approach, *Journal of Climate*, 33, 6297–6314, 2020.

Rivero-Calle, S., Gnanadesikan, A., Del Castillo, C. E., Balch, W. M., and Guikema, S. D.: Multidecadal increase in North Atlantic coccolithophores and the potential role of rising CO<sub>2</sub>, *Science*, 350, 1533–1537, 2015.

625 Rousi, E., Kornhuber, K., Beobide-Arsuaga, G., Luo, F., and Coumou, D.: Accelerated western European heatwave trends linked to more-persistent double jets over Eurasia, *Nature communications*, 13, 3851, 2022.

Sallée, J.-B., Pelichero, V., Akhoudas, C., Pauthenet, E., Vignes, L., Schmidtko, S., Garabato, A. N., Sutherland, P., and Kuusela, M.: Summertime increases in upper-ocean stratification and mixed-layer depth, *Nature*, 591, 592–598, 2021.

630 Sandø, A. B., Nilsen, J. Ø., Gao, Y., and Lohmann, K.: Importance of heat transport and local air-sea heat fluxes for Barents Sea climate variability, *Journal of Geophysical Research: Oceans*, 115, 2010.

Santana-Falcón, Y. and Séférian, R.: Climate change impacts the vertical structure of marine ecosystem thermal ranges, *Nature Climate Change*, 12, 935–942, 2022.

635 Santana-Falcón, Y., Yamamoto, A., Lenton, A., Jones, C. D., Burger, F. A., John, J. G., Tjiputra, J., Schwinger, J., Kawamiya, M., Frölicher, T. L., et al.: Irreversible loss in marine ecosystem habitability after a temperature overshoot, *Communications Earth & Environment*, 4, 343, 2023.

Schlüter, L., Lohbeck, K. T., Gutowska, M. A., Gröger, J. P., Riebesell, U., and Reusch, T. B.: Adaptation of a globally important coccolithophore to ocean warming and acidification, *Nature Climate Change*, 4, 1024–1030, 2014.

640 Sen Gupta, A., Thomsen, M., BenthuySEN, J. A., Hobday, A. J., Oliver, E., Alexander, L. V., Burrows, M. T., Donat, M. G., Feng, M., Holbrook, N. J., et al.: Drivers and impacts of the most extreme marine heatwave events, *Scientific reports*, 10, 19 359, 2020.

Shutler, J., Grant, M., Miller, P., Rushton, E., and Anderson, K.: Coccolithophore bloom detection in the north east Atlantic using SeaWiFS: Algorithm description, application and sensitivity analysis, *Remote Sensing of Environment*, 114, 1008–1016, 2010.

645 Simon, A., Poppeschi, C., Plecha, S., Charria, G., and Russo, A.: Coastal and regional marine heatwaves and cold spells in the northeastern Atlantic, *Ocean Science*, 19, 1339–1355, 2023.

Smale, D. A., Wernberg, T., Oliver, E. C., Thomsen, M., Harvey, B. P., Straub, S. C., Burrows, M. T., Alexander, L. V., BenthuySEN, J. A., 650 Donat, M. G., et al.: Marine heatwaves threaten global biodiversity and the provision of ecosystem services, *Nature Climate Change*, 9, 306–312, 2019.

Smith, H. E., Poulton, A. J., Garley, R., Hopkins, J., Lubelczyk, L. C., Drapeau, D. T., Rauschenberg, S., Twining, B. S., Bates, N. R., and Balch, W. M.: The influence of environmental variability on the biogeography of coccolithophores and diatoms in the Great Calcite Belt, *Biogeosciences*, 14, 4905–4925, 2017.

655 Smith, K. E., Burrows, M. T., Hobday, A. J., Sen Gupta, A., Moore, P. J., Thomsen, M., Wernberg, T., and Smale, D. A.: Socioeconomic impacts of marine heatwaves: Global issues and opportunities, *Science*, 374, eabj3593, 2021.

Smith, K. E., Burrows, M. T., Hobday, A. J., King, N. G., Moore, P. J., Sen Gupta, A., Thomsen, M. S., Wernberg, T., and Smale, D. A.: Biological impacts of marine heatwaves, *Annual Review of Marine Science*, 15, 119–145, 2023.

Smyth, T. J., Moore, G. F., Groom, S. B., Land, P. E., and Tyrrell, T.: Optical modeling and measurements of a coccolithophore bloom, 660 Applied Optics, 41, 7679–7688, 2002.

Stott, P. A., Christidis, N., Otto, F. E., Sun, Y., Vanderlinden, J.-P., van Oldenborgh, G. J., Vautard, R., von Storch, H., Walton, P., Yiou, P., et al.: Attribution of extreme weather and climate-related events, *Wiley Interdisciplinary Reviews: Climate Change*, 7, 23–41, 2016.

Swart, N. C., Fyfe, J. C., Hawkins, E., Kay, J. E., and Jahn, A.: Influence of internal variability on Arctic sea-ice trends, *Nature Climate Change*, 5, 86–89, 2015.

665 Terhaar, J., Kwiatkowski, L., and Bopp, L.: Emergent constraint on Arctic Ocean acidification in the twenty-first century, *Nature*, 582, 379–383, 2020.

Terhaar, J., Burger, F. A., Vogt, L., Frölicher, T. L., and Stocker, T. F.: Record sea surface temperature jump in 2023–2024 unlikely but not unexpected, *Nature*, pp. 1–5, 2025.

Tyrrell, T., Holligan, P., and MobleY, C.: Optical impacts of oceanic coccolithophore blooms, *Journal of Geophysical Research: Oceans*, 104, 3223–3241, 1999.

Von Schuckmann, K., Cheng, L., Palmer, M. D., Tassone, C., Aich, V., Adusumilli, S., Beltrami, H., Boyer, T., Cuesta-Valero, F. J., Desbruyères, D., et al.: Heat stored in the earth system: Where does the energy go? The GCOS earth heat inventory team, *Earth System Science Data Discussions*, 2020, 1–45, 2020.

Werdell, P. J., Behrenfeld, M. J., Bontempi, P. S., Boss, E., Cairns, B., Davis, G. T., Franz, B. A., Gliese, U. B., Gorman, E. T., Hasekamp, O.,  
670 et al.: The plankton, aerosol, cloud, ocean ecosystem mission: Status, science, advances, *Bulletin of the American Meteorological Society*, 100, 1775–1794, 2019.

Wernberg, T., Thomsen, M. S., Burrows, M. T., Filbee-Dexter, K., Hobday, A. J., Holbrook, N. J., Montie, S., Moore, P. J., Oliver, E. C.,  
Sen Gupta, A., et al.: Marine heatwaves as hot spots of climate change and impacts on biodiversity and ecosystem services, *Nature Reviews Biodiversity*, pp. 1–19, 2025.

675 Winter, A., Henderiks, J., Beaufort, L., Rickaby, R. E., and Brown, C. W.: Poleward expansion of the coccolithophore *Emiliania huxleyi*, *Journal of Plankton Research*, 36, 316–325, 2014.

Wunderling, N., von der Heydt, A. S., Aksenov, Y., Barker, S., Bastiaansen, R., Brovkin, V., Brunetti, M., Couplet, V., Kleinen, T., Lear, C. H., et al.: Climate tipping point interactions and cascades: a review, *Earth System Dynamics*, 15, 41–74, 2024.

Zscheischler, J., Westra, S., Van Den Hurk, B. J., Seneviratne, S. I., Ward, P. J., Pitman, A., AghaKouchak, A., Bresch, D. N., Leonard, M.,  
680 Wahl, T., et al.: Future climate risk from compound events, *Nature climate change*, 8, 469–477, 2018.